

**Discovery of a Suppressor of ADF1 and the
Mapping of a new ADF gene, ADF2, in
*Chlamydomonas reinhardtii***

by

Julie Coralina Rodriguez Pike

B.Sc. (Molecular Biology & Biochemistry), Simon Fraser University, 2010

Thesis Submitted In Partial Fulfillment of the
Requirements for the Degree of
Master of Science

In the
Department of Molecular Biology and Biochemistry
Faculty of Science

© **Julie Rodriguez 2013**

SIMON FRASER UNIVERSITY

Summer 2013

All rights reserved.

However, in accordance with the *Copyright Act of Canada*, this work may be reproduced, without authorization, under the conditions for "Fair Dealing." Therefore, limited reproduction of this work for the purposes of private study, research, criticism, review and news reporting is likely to be in accordance with the law, particularly if cited appropriately.

Approval

Name: Julie Coralina Rodriguez Pike

Degree: Master of Science

Title of Thesis: Discovery of a Suppressor of ADF1 and the Mapping of a new ADF gene, ADF2, in *Chlamydomonas reinhardtii*

Examining Committee: **Chair:** Dr. Jonathan Choy
Assistant Professor of Molecular Biology and Biochemistry

Dr. Lynne M. Quarmby
Senior Supervisor
Chair of the Molecular Biology and
Biochemistry Department

Dr. Nancy Hawkins
Supervisor
Associate Professor of Molecular Biology
and Biochemistry

Dr. Michel R. Leroux
Supervisor
Professor of Molecular Biology and
Biochemistry

Dr. Jae-Hyeok Lee
Internal Examiner
Assistant Professor
UBC/Department of Botany

Date Defended/Approved: July 24th 2013

Partial Copyright License



The author, whose copyright is declared on the title page of this work, has granted to Simon Fraser University the right to lend this thesis, project or extended essay to users of the Simon Fraser University Library, and to make partial or single copies only for such users or in response to a request from the library of any other university, or other educational institution, on its own behalf or for one of its users.

The author has further granted permission to Simon Fraser University to keep or make a digital copy for use in its circulating collection (currently available to the public at the "Institutional Repository" link of the SFU Library website (www.lib.sfu.ca) at <http://summit/sfu.ca> and, without changing the content, to translate the thesis/project or extended essays, if technically possible, to any medium or format for the purpose of preservation of the digital work.

The author has further agreed that permission for multiple copying of this work for scholarly purposes may be granted by either the author or the Dean of Graduate Studies.

It is understood that copying or publication of this work for financial gain shall not be allowed without the author's written permission.

Permission for public performance, or limited permission for private scholarly use, of any multimedia materials forming part of this work, may have been granted by the author. This information may be found on the separately catalogued multimedia material and in the signed Partial Copyright Licence.

While licensing SFU to permit the above uses, the author retains copyright in the thesis, project or extended essays, including the right to change the work for subsequent purposes, including editing and publishing the work in whole or in part, and licensing other parties, as the author may desire.

The original Partial Copyright Licence attesting to these terms, and signed by this author, may be found in the original bound copy of this work, retained in the Simon Fraser University Archive.

Simon Fraser University Library
Burnaby, British Columbia, Canada

revised Fall 2011

Abstract

Eukaryotic cilia are evolutionary conserved microtubule-based organelles that play important roles in cell signalling, development and motility. Cilia can be shed through a process known as deflagellation, in which the cilium is severed at a specific site at its base in response to a stress signal, through calcium signalling. Fifteen years ago three genes were uncovered in a screen for deflagellation mutants, two of which were cloned and their roles in the microtubule-severing event characterized. The third gene, named ADF1 has to date eluded identification. A previous graduate student genetically mapped ADF1 to Linkage Group (Chromosome) IX to identify the ADF1 gene. I tried, unsuccessfully, to rescue the *adf1* mutation with wild type DNA from the gene locus. In the rescue attempts I recovered a potential suppressor of the *adf1-3* mutant. Despite the many attempts I was unable to rescue *adf1* or identify the flanking DNA of the *adf1-3* suppressor. Since no MT severing protein or calcium sensor were recovered in the original genetic screen a second genetic screen is being carried out, this time for conditional deflagellation mutants. From this screen I characterized a new acid induced deflagellation gene, ADF2, and mapped it to Linkage Group III. The work in this thesis thus contributes new information about two previously unknown deflagellation genes, ADF2 and ADF1-Suppressor.

Keywords: Cilia; Deflagellation; *Chlamydomonas reinhardtii*; ADF1; ADF2

To my family and friends

Acknowledgements

I would like to acknowledge everyone who worked and helped me on the ADF1 project: Jaime Kirschner, Courtney Choutka, Adam Staniscia, Vy Tran, and Kavisha Gunadarwane. I would also like to thank the ADF2 team: Freda Warner, Fabian Garces, Fabian Meili, Paul Buckoll, Mihajlo Todorovic and Mette Lethan. Thank-you to my supervisor Lynne Quarmby for giving me the opportunity to do research; you have been a great mentor throughout these years. I would also like to acknowledge my supervisory committee Michel Leroux and Nancy Hawkins, for all the help and advice given on what has been an ongoing struggle with ADF1. Finally I would like to thank Laura Hilton: you have been an amazing friend and mentor these last four years, there were times when I couldn't have done this without you (both for ADF1 and ADF2) and I will miss working with you.

Table of Contents

Approval.....	ii
Partial Copyright Licence	iii
Abstract.....	iv
Dedication.....	v.
Acknowledgements.....	vi
Table of Contents.....	vi
List of Tables.....	ix
List of Figures.....	x
Glossary.....	xii
1. Introduction	1.
1.1. Cilia	1.
1.2. Ciliary Disassembly	3.
1.3. Acid Induced Deflagellation	6.
1.4. Deflagellation Genetic Screen: 1998	11.
References.....	22.
2. ADF1: The acid deflagellation gene 1	28.
2.1. Linkage Analysis map of ADF1.....	28.
2.2. Rescuing ADF1	30.
2.3. The search for PAR.....	35.
2.4. Conclusion	39.
Supplemental Data.....	54.
References.....	60.
3. ADF2: The acid deflagellation gene 2	61.
3.1. A new Deflagellation Genetic Screen and a new ADF gene	61.
3.2. Linkage Analysis of ADF2.....	63.
3.3. Conclusion	65.
References.....	76.
4. Discussion	77.
4.1. ADF1.....	78.
4.2. ADF2.....	80.
References.....	84.
5. Materials and Methods.....	86.
5.1. Strains and Growth Conditions	86.
5.2. BAC DNA & Plasmid Preparations	86.
5.3. Sub-cloning for Phenotypic Rescue Assays and for Sequencing	86.
5.4. <i>Chlamydomonas</i> Transformations	87.
5.5. Deflagellation Assays	87.
5.6. Genetic Crosses.....	88.
5.7. Genomic DNA Isolation from <i>Chlamydomonas</i>	88.

5.8. Southern Blots.....	89.
5.9. TAIL-Adaptor PCR.....	90.
5.10. Self-Ligation PCR.....	90.
5.11. Bacterial Transformations.....	91.
5.12. Colony Lifts	91.
5.13. PCR-based Recombination Frequency Mapping	92.
References.....	93.
Appendices.....	94
Appendix A. Strains used in this study.....	95
Appendix B. The BACs spanning the ADF1 locus	96
Appendix C. Primers used in the ADF1 Analysis	97
Appendix D. Molecular Markers for ADF2 Linkage Analysis	98

List of Tables

Table 1-1. The Deflagellation mutants identified in the 1998 Genetic Screen.....	21.
Table 3-1. The Deflagellation Mutants Recovered in the 2012 Conditional Genetic Screen.....	68.
Table 3-2. Linkage Analysis of the progeny from the nine <i>adf2-1/S1D2</i> zygotes.....	72.
Table 3-3. Linkage Analysis of the 63 progeny from the <i>adf2-1/S1D2</i> bulk-zygote analysis	74.
Table 4-1. Genes up-regulated during Ciliogenesis in the ADF2 gene locus.....	83.

List of Figures

Figure 1-1. Schematic of a typical motile cilium (flagellum)	15.
Figure 1-2. The model organism <i>Chlamydomonas reinhardtii</i> and its two flagella	16.
Figure 1-3. Schematic comparing the two modes of Ciliary Disassembly	17.
Figure 1-4. Transition electron micrographs of deflagellation in <i>Chlamydomonas</i>	18.
Figure 1-5. Schematic diagram of the Signalling Pathway for Acid-Induced Deflagellation.....	19.
Figure 1-6. The Deflagellation mutant Phenotypes.....	20.
Figure 2-1. The <i>Chlamydomonas</i> life cycle	41.
Figure 2-2. Linkage analysis of the ADF1 region.....	42.
Figure 2-3. The ADF1 gene locus	43.
Figure 2-4. ADF1 Phenotypic Rescue Assays.....	44.
Figure 2-5. BAC24I14 Gene Predictions	45.
Figure 2-6. Southern analysis reveals single gene copy of two BAC24I14 fragments in the genome of the <i>adf1-3</i> rescue strain	46.
Figure 2-7. The PAR insertion site in the <i>adf1-3</i> rescue strain.....	47.
Figure 2-8. The Self-ligation PCR method.....	48.
Figure 2-9. Self-ligation PCR identified a piece of BAC24I14 beside the PAR insertion in the original <i>adf1-3</i> strain not associated with the rescuing deflagellation phenotype	49.
Figure 2-10. The TAIL-Adaptor PCR method.....	50.
Figure 2-11. TAIL-Adaptor PCR amplified a ~1.3kb band from the 6.5kb SmaI PAR insertion site	51.
Figure 2-12. The Colony Lift method	52.
Figure 2-13. Colony lifts were used to try and identify bacteria containing constructs with the PAR insertion sites	53.
Figure S2-1. pSI103	54.
Figure S2-2. The PAR insertion sites generated in the PAR Southern Blot.....	55.

Figure S2-3. The Self-ligation PCR product from the 6.5kb SmaI PAR insertion site.....	56.
Figure S2-4. The Self-ligation PCR method amplified a fragment of BAC24I4 in the original <i>adf1-3</i> rescue strain using a PAR specific primer	57.
Figure S2-5. The Self-ligation PCR method amplified a fragment of BAC24I14 in the original <i>adf1-3</i> rescue strain using an AMP specific primer	58.
Figure S2-6. The TAIL-Adaptor PCR method generated a 1.3kb product, which appeared to be sub-cloned into pGEMT	59.
Figure 3-1. Complementation analysis in dikaryons reveals a new gene, ADF2, involved in the calcium-signalling step in Deflagellation	69.
Figure 3-2. Linkage analysis places ADF2 on chromosome 3.....	70.
Figure 3-3. Linkage analysis places ADF2 either: (1) between markers 2A and 7.4A or (2) between markers 8B and 9A	71.
Figure 4-1. LG III molecular and genetic markers.....	82.

Glossary

Cilia	Microtubule-based organelles that extend/protrude from the cell; can be motile or immotile; in Eukaryotes the term cilia and flagella are used interchangeably
Deflagellation	The severing of the outer microtubules that make up the axoneme (core) of the cilium/flagellum in response to stress; also known as deciliation or flagellar autotomy
Transition Zone	The region of the cilium where the basal body microtubules are exchanged for the microtubules, which make up the axoneme. It is thought to contain proteins that regulate entry of proteins into the flagellum
Linkage Analysis	Method used to create a linkage or genetic map- where the positions of genes or genetic markers are determined based on recombination frequencies. Also known as genetic analysis/mapping or PCR-based recombination frequency mapping.
Molecular Marker	A fragment of DNA heterozygosity, used as a label for a known chromosomal locus.

1. Introduction

1.1 Cilia

Cilia were once believed to function solely in motility; however, recent research has shown cilia to be important sensory organelles participating in signal transduction and cell cycle control (reviewed by Christensen et al., 2007). Defects in ciliary structure and function have further revealed their importance as these defects cause an array of disorders known as ciliopathies (Hilderbrandt et al., 2011). Nearly all eukaryotic cells are ciliated with the exception of most fungi and plants, which have independently lost them (James et al., 2006; Wickstead & Gull, 2007).

The ubiquitous presence of cilia highlights their deep evolutionary history and the significance of the cellular roles they play, functioning as motile and/or sensory organelles. In humans cilia are present in almost all cell lineages (Wheatley, 1995; Wheatley et al., 1996). They are found in the photoreceptor cells of the eye where a highly specialized cilium, known as the connecting cilium, joins the light sensing outer segment to the cell body (inner segment) (Estrada-Cuzcano et al., 2012). In olfactory neurons cilia are found at the ends of the axons lining the air ducts (Tadenev et al., 2011). They are also found in the brain ventricles, are important in both the male and female reproductive systems, and are crucial signalling organelles during embryonic development, helping to establish left/right asymmetry (Kishimoto & Sawamoto, 2012; Pier et al., 2013; Badu & Roy, 2013).

The cilium, or eukaryotic flagellum, is highly conserved both at the protein and ultrastructure level. It has four defined zones: the basal body (BB), the transition zone (TZ), the cilium proper, and the ciliary tip (Figure 1-1). The basal bodies, which are composed of nine outer triplet microtubules function as anchors from which the cilium's core, or axoneme, extends. At the transition zone, the triplet microtubules are converted for doublets arranged in a ring forming the axoneme and cilium proper. This ring of microtubules can enclose a pair of central microtubules yielding a 9+2 ciliary structure, where the central pair with its associated protein/complexes regulates axonemal bending. In primary cilia, or non-motile cilia, the central pair is absent forming a 9+0 arrangement.

The flagellar axoneme is enclosed by a membrane, which is continuous but distinct from the plasma membrane, and is the home to many signal transduction players. Cilia have been shown to be involved in Sonic Hedgehog (Shh) signalling (Mukhopadhyay et al., 2013; Willaredt et al., 2012), the planar cell polarity (PCP) pathway (Veland et al., 2013; Wang and Nathans, 2007) and WNT signalling (Lienkamp et al., 2012). They are also involved in chemo-, photo- and mechano- sensing, G-protein coupled signalling in olfactory cells, somatostatin & serotonin signalling in neuronal cilia and in establishing left/right asymmetry during development (Manning et al., 2013). Ciliary NIMA-related kinases (NEKs) have also been implicated as mediators of the cell cycle (Quarmby and Parker, 2005).

Due to the diverse roles that they play it is not surprising that defects in cilia result in a spectrum of diseases and disorders. In both polycystic kidney disease (PKD) and nephronophthisis (NPHP) ciliary signalling is disrupted resulting in cyst formation (Ko and Park, 2013; Kotsis et al., 2013). Defects in components of ciliary assembly and function have been identified to cause disorders such as: primary cilia dyskinesia, Meckel-Gruber

Syndrome, Bardet-Biedl syndrome, Alstrom syndrome, Joubert syndrome and Orfaciodigital syndrome (reviewed by Inglis et al., 2006) and has also been implicated in obesity, blindness and deafness (Berbari et al., 2013; Mukhopadhyay and Jackson, 2011).

There are several model organisms used to study both primary and motile cilia. One good model organism used to study motile cilia is the unicellular green alga *Chlamydomonas reinhardtii* (Figure 1-2). *C.reinhardtii* is a motile single-celled alga. It is bi-flagellated and uses its flagella for motility, sensing its environment, numerous signal transduction pathways and for mating. Due to high evolutionary conservation, *C.reinhardtii* flagella have been used for decades to study the function of human orthologs of ciliary proteins. The ability to deflagellate *C.reinhardtii* cells (by the use of a weak organic acid), releasing the flagella from the cell body without killing the cells, has allowed us to study the process of flagellar assembly. Other advantages that make *C.reinhardtii* an effective model organism is that its nuclear genome has been sequenced and annotated, a flagellar proteome has been assembled, use of haploid genetics, biochemical purification and fractionation of flagella are easily performed and cell models (detergent-extracted cells) can be generated and used for *in vitro* experiments. The research focus of the Quarmby lab is to study how cilia disassemble in the model organism *C.reinhardtii*, which will be from hereon referred to as *Chlamydomonas*.

1.2 Ciliary Disassembly

Ciliary disassembly occurs in either one of two ways: either through reabsorption of the cilium back into the cell prior to mitosis, or through deflagellation, the severing of the

cilium in response to physical or chemical stress (Figure 1-3). Reabsorption is a slow process in which the length of the flagellum gradually shortens as it is disassembled from the tip down prior to cell division (Cavalier-Smith, 1974). It also occurs in quadriflagellate cells shortly after mating and when cells are transferred to solid media (Marshall and Rosenbaum 2001; Laura Hilton, unpublished). Several pharmacological agents such as the phosphodiesterase inhibitor IBMX, which inhibits assembly allowing for constitutive disassembly, and sodium pyrophosphate, through an unknown pathway, can also induce flagellar reabsorption (Wilson et al., 2008; Quader et al., 1978).

In contrast, deflagellation, also known as deciliation or flagellar autotomy, is the severing and release of the cilium due to a stress signal. This severing occurs at a specific site distal to the transition zone known as the site of flagellar autotomy (Figure 1-4). It is unknown why this process occurs, for free-living ciliates, such as *Chlamydomonas*, it has been hypothesized that deflagellation provides a survival advantage (Lewin et al., 1982). Though cilia are membrane enclosed, the cell wall does not encompass it, thus, it remains exposed to the environment. In this hypothesis, the shedding of the flagella reduces the surface area of the cell exposed to an unfavourable physiochemical environment. It has also been seen that when their flagella is trapped by predators *Chlamydomonas* cells deflagellate allowing the cell body to float away (Pickett-Heaps and Pickett Heaps, 1996). Though this hypothesis may work for free-living ciliates it does not explain deflagellation events in: sea urchin embryos (Casano et al., 2003), mice kidney cells (Kim et al., 2013), nasal epithelia (Maier et al., 2012), olfactory cilia in zebrafish (Friedrich and Korsching, 1997) and rat brain ependymal cells (Mohammed et al., 1999).

Due to the ubiquitous nature of deflagellation in both uni- and bi-flagellated cells, and the conservation of the flagellar structure, it is likely that the mechanism of ciliary autotomy

is also conserved and was present in the ancestral ciliated eukaryote (Quarmby, 2009). The severing site in deflagellation then could be an outcome of the way that flagella are built (Blum, 1971), a consequence of their evolutionary history and not a selected trait (Quarmby, 2004). In this theory the flagellar break point plays a more fundamental role in the cell. One possibility is that deciliation facilitates reabsorption of the flagellum prior to cell division releasing the basal bodies for spindle organization. Though a controversial idea, it has been shown that *Chlamydomonas* cells do sever their transition zones following reabsorption (Parker et al., 2010). Deflagellation, thus, could be the hyperactivation of disassembly that in certain species has been selected as adaptive behaviours, in which cells shed the flagella in order to free the basal bodies. If this is true then studying deflagellation could not only give us insight into the individual adaptive roles it plays in different organisms but also allow us to further understand how cells undergo and regulate cell division and the cell cycle.

Deflagellation can be induced by various stimuli, such as dibucaine, mastoporan, weak organic acids, temperature and mechanical shear. In all of these instances the mechanism of deciliation is calcium dependent where the presence of extracellular calcium is required for the severing of the flagellar axoneme, following reception of the stress signal (Reviewed in Quarmby, 2009). Dibucaine, a local anaesthetic, is lipophilic and targets many membrane proteins, it has been proposed that dibucaine may affect specific membrane proteins or lipids involved in calcium regulation (Catterall, 1992; Antenedo et al., 1994). The wasp venom, mastoporan, on the other hand is a general activator of heterotrimeric G-proteins and it has been suggested that deflagellation occurs through phospholipase C activity (Kuin et al., 2000; Quarmby et al., 1992). Severe mechanical shear has also been shown to induce deflagellation (Rosenbaum and Child, 1967), this

process requires calcium and is thought to trigger normal calcium-induced severing as cells can recover and regenerate their flagella. High temperature also induces deflagellation but the mechanism involved is not known (Lewin et al., 1982). Given that deflagellation is calcium dependent, it is likely that excision is triggered by an increase in intracellular calcium at the transition zone where severing occurs. To comprehend the signalling pathway(s) involved in this ciliary disassembly process acid-induced deflagellation was selected because the mechanism has been shown to increase intracellular calcium (Quarmby et al., 1992). The following section discusses the signalling pathway of acid induced deflagellation, which is the focus of my thesis.

1.3 Acid Induced Deflagellation

Originally employed to isolate intact cilia for biochemical analysis, pH shock has been found to induce deflagellation by intracellular acidification and activation of a calcium influx (Quarmby, 2004). This mechanism is not the result of a fast drop in the extracellular pH nor can strong acids induce it. It is mediated by weak organic acids, which are protonated and can permeate the cell membrane (Figure 1-5). Once inside the cell the acid deprotonates, resulting in a decrease in intracellular pH activating an influx of extracellular calcium.

This calcium requirement was established when cells failed to deflagellate in the absence of calcium (Quarmby and Hartzell, 1994). Cells treated with benzoate without calcium remained flagellated but were able to deflagellate if calcium was added subsequently. To further analyze the importance of the calcium influx ^{45}Ca influx assays

were performed on cells treated with acid (benzoate) and the Ca^{2+} channel blockers Cadmium (Cd^{2+}) and Lanthanum (La^{3+}). These assays revealed that there are two phases to acid-induced calcium influx: an initial rapid phase followed by a prolonged phase. Using calcium indicator dyes, elevated calcium was found to initially localize to the apical end of the cell, at the base of the flagellum, during the rapid influx phase (Wheeler et al., 2008). Following the initial calcium influx, whole cell elevation of cytosolic calcium was observed, purportedly comprising the prolonged phase.

The calcium influx pathway is thought to localize to the flagellar transition zone at the base of the flagellum where excision occurs. Support for this comes from *in vitro* deflagellation experiments performed on *Chlamydomonas* flagellar-basal body complexes (FBBCs) (Lohret et al., 1998). These FBBCs can deflagellate in the presence of 1 μM calcium, indicating that everything downstream of calcium in the signalling pathway is integral to the axoneme. Consistent with this is the fact that the initial rapid influx phase localizes to the base of the flagella (Wheeler et al., 2008), and is lost following deflagellation but recovered after flagella are re-grown (Quarmby, 1996).

Though acid-induced deflagellation is calcium dependent research indicates that the extracellular calcium that enters the cell during the influx step is not the calcium responsible for activating the microtubule severing machinery. When placed in media containing Strontium (Sr^{2+}), a divalent cation similar to calcium, whole cells were able to deflagellate in response to acid (Evans et al., 1997). However, Sr^{2+} failed to induce axonemal severing in detergent permeabilized cell models, while calcium alone can (Sanders and Salisbury, 1994), indicating that there is a second calcium source (released from an intracellular store), which activates the microtubule severing machinery.

Consistent with the presence of a second calcium source it has been shown that in both acid- and mastoporan- induced deflagellation inositol phospholipid metabolism is activated through the activation of phospholipase C (PLC) (Kuin et al., 2000; Quarmby et al., 1992). Activation of PLC could thus lead to the release of intracellular calcium stores from the ER through the classical pathway, where PLC hydrolyses PtdIns(4,5)P₂ into diacylglycerol and Ins(1,4,5)P₃, which then binds to its receptor on the ER membrane and causes the release of calcium into the cytosol. This theory is supported by the fact that Neomycin, a phospholipase C inhibitor, blocked both the acid-induced increase of Ins(1,4,5)P₃ and deflagellation (Quarmby et al., 1992). This data suggests that the extracellular calcium that influxes into the cell, through activation of unknown protein(s) (potentially a G-protein) may activate phospholipase C resulting in the release of calcium from an IP₃ sensitive intracellular store. This intracellular calcium is then responsible for activating the microtubule severing machinery, allowing for deflagellation to occur.

Deflagellation results in the severing of the outer doublet axonemal microtubules. Unlike free microtubules axonemal microtubules are highly stabilized by the components that make up the flagella, making it difficult for the axoneme to come apart (i.e. be severed). There are few known proteins that sever microtubules most of which are AAA-ATPases, members of the P-Loop NTPase superfamily. These ATPases couple chemical energy, from ATP hydrolysis, to mechanical force, exerting it for the translocation or remodelling of macromolecules. Katanin, Spastin, Fidgetin and VPS4 comprise a small subgroup of AAA-ATPases that have been found to sever microtubules (Reviewed by Roll-Mecak and McNally, 2010). These ATPases are composed of a highly conserved AAA domain at the C-terminus that binds and hydrolyzes ATP. The N-terminus contains a Microtubule Interacting and Trafficking domain (MIT), allowing the protein to bind to

microtubules with low affinity. VPS4 does not itself sever microtubules but instead is responsible for disassembling protein complexes involved in membrane trafficking. Spastin and Fidgetin are Katanin related ATPases, which do sever microtubules. All of these AAA-ATPases are found in *Chlamydomonas* with the exception of Spastin.

Katanin and Spastin are the most well studied AAA-ATPases from the subgroup. When bound to ATP they bind with high affinity to microtubules forming ring-shaped hexamers; the mechanism by which they sever microtubules is not understood. Katanin is a heterodimer composed of a p60 (60kD) subunit, containing the AAA domain (Lohret et al., 1999), and a p80 (80kD) subunit, believed to be a regulatory domain necessary for p60 dimerization and localization (McNally et al., 2000). Though Katanin requires ATP *in vitro* to sever microtubules, isolated flagellar basal body complexes (FBBCs) sever at the transition zone in response to calcium alone (Lohret et al., 1998). In this system exogenous ATP is not required. Thus if Katanin is the microtubule severing protein during deflagellation then it must be pre-loaded on axonemal microtubules bound to ATP.

Chlamydomonas contains two katanin genes, KAT1 and KAT2, as well as a Fidgetin and VPS4 homolog. Using EM immunogold staining and a human specific p60 antibody, the KAT1 p60 subunit was shown to localize to the basal bodies, distal striated fibres and both the distal and proximal ends of the transition zone (Lohret et al., 1999). The p60 subunit is able to sever not only isolated microtubules but also the axonemal microtubules of flagella in whole cells (cells incubated with purified p60 in the presence of ATP) and in isolated FBBCs (Lohret et al., 1998). The study also showed that the human-p60 antibody could block endogenous katanin in isolated FBBCs, supporting a role for katanin as the microtubule severing protein in deflagellation.

Katanin's role in axonemal microtubule severing is controversial. In 2009 Qasim Rasi, a graduate student in the Quarmby lab, implicated KAT1 p60 as the microtubule severing protein involved in deflagellation and in pre-mitotic reabsorption (Rasi et al., 2009). In this study Qasim found that knockdown of katanin p60 through RNA interference (RNAi) in *Chlamydomonas* was only possible in strains defective in ciliogenesis where cilia were unable to grow. Furthermore, it was found that knockdown of p60 in a cell wall-less background (where the flagella are only retained if anchored to basal bodies) caused cellular abnormalities and retention of flagella during cell division, potentially indicating a role for katanin in pre-mitotic ciliary disassembly. However, in 2012 the paralyzed flagellar mutant *pf19* was found to carry a mutation in the p60 subunit of KAT1 (Dymek and Smith, 2012). Though the mutation was discovered to abolish p60's ability to sever microtubules *in vitro*, the *pf19* mutant retained the ability to deflagellate in response to acid and to sever during pre-mitotic reabsorption. The same results were observed in amiRNA (artificial micro RNAs) p60 katanin knockdowns. Based on their data, the authors concluded that KAT1 p60 must not be involved in either process. These conflicting results can be resolved by looking at the technique used by Qasim to knockdown the p60 gene. Though it was the best technique at the time, RNAi has since been shown to produce off-target effects. It is therefore likely that Qasim's RNAi construct could have knockdown one of the other p60 genes in *Chlamydomonas*, such as KAT2 p60. Thus, while KAT1 p60 may not be involved in deflagellation or pre-mitotic severing, it is still possible that katanin is the protein responsible for flagellar excision.

So how do we identify the genes involved in deflagellation? The classic approach in discovering genes in pathways is to mutagenize a population of cells and then selectively recover the mutants involved in the pathway based on their phenotype. Genetic mapping

and/or bioinformatics can then be performed to identify the mutated gene. Using this approach a flagellar autotomy mutant, unable to deflagellate in response to acid, was generated through UV-mutagenesis (Lewin and Burrascano et al., 1983). This mutant, *fa1*, is also unable to deflagellate in the presence of detergent, which bypasses the calcium-signalling pathway (Figure 1-6). A second deflagellation mutant was later discovered as a second unlinked mutation carried by the mating defective *imp4* mutant (T. Saito and U. Goodenough, Washington University, St. Louis). This second mutant, *adf1*, fails to deflagellate in response to acid but will in the presence of detergent and calcium. Based on the *adf* and *fa* phenotypes deflagellation can be broken down into two parts: (1) the proton-activated calcium-signalling pathway, which is defective in the *adf1* mutant, and (2) axonal severing by the microtubule severing machinery, which is blocked in the *fa1* strain.

1.4 Deflagellation Genetic Screen: 1998

To identify the genes involved in the deflagellation pathway a genetic screen was performed by the Quarmby lab (Finst et al., 1998). The screen recovered thirteen mutants defective in deflagellation: five displaying the *adf* phenotype and eight with the *fa* phenotype (Table 1-1). To determine if the five new mutants with the *adf* phenotype were allelic to *adf1*, the mutants were all crossed to *adf1* and the progeny tested for deflagellation. The progeny from all crosses with *adf1* exhibited the *adf* phenotype suggesting that they are alleles of *adf1*. This was confirmed by complementation tests on stable diploids (all diploids were *adf* for deflagellation). The same characterization was performed for the mutants with the *fa* phenotype. Four of the mutants were found to be alleles of the original *fa1* mutant, while the other four mutants were found to be alleles of

each other. Thus, the *fa* mutants define two genes: the original FA1 gene and a novel FA2 gene.

Deflagellation was also tested in wild type (WT) /mutant stable diploids for *adf1*, *fa1* and *fa2*. In all cases the diploids deflagellated indicating that all of the alleles for the three genes are recessive. To test if the WT components of deflagellation could rescue the *adf* and *fa* mutations complementation analysis was performed on dikaryons. *Chlamydomonas* cells spend most of their lives as haploids, however dikaryons are temporarily formed during sexual reproduction shortly after the cells fuse, where the fused cell retains both separate nuclei and both set of flagella. These dikaryons can be used to see if the flagellar or cellular components from the WT cell can rescue mutant preformed complexes and structures. For the *ADF/adf* dikaryons two of the flagella were shed right away after deflagellation induction (acid treatment). After 30 minutes the remaining pair of flagella were also shed from the cell. Thus, the deflagellation machinery of the WT gamete can rescue the *adf* phenotype. This rescue event was found to not require protein synthesis, indicating that the WT components are sufficient to restore deflagellation in the *adf1* mutant. The same experiments were carried out with the *fa* mutants. For both *fa1* and *fa2* mutants only the WT flagella were able to deflagellate, thus the *fa* mutations cannot be rescued by the WT cytoplasm in dikaryons.

To identify the genes encoded by *fa1*, *fa2* and *adf1* alleles for all three generated through insertional mutagenesis were further analyzed. Using radioactively labeled probes for the insertional marker the insertion sites of the marker were identified for *fa1* and *fa2*. Using subsequent genetic mapping and complementation analysis, the FA1 gene was found to encode a 171kDa protein with predicted coiled-coil and Ca²⁺/Calmodulin binding domains (Finst et al., 2000). Biochemical fractionation indicates that Fa1p associates with

the transition zone since it is only found in the flagellar basal body complex and not in the axoneme, which was later confirmed through immunofluorescence (Jeremy Parker, unpublished). FA1 mutants have also been shown to have defects in pre-mitotic flagellar reabsorption (slow) and are slow to regrow flagella after mitosis (Quarmby, 2009).

FA2 encodes a NIMA-related kinase (NEK) with an IKSAN motif in the catalytic domain suggesting that it is a serine/threonine kinase (Mahjoub et al., 2002). These mutant cells also have defects in pre-mitotic reabsorption (slow) and also regrow their flagella slowly after mitosis. FA2 mutants were also found to have a delay in entering mitosis causing the cells to be larger in size prior to cell division. Indirect immunofluorescence reveals that Fa2p localizes to the basal bodies and, like FA1, to the distal end of the transition zone where deflagellation occurs (Mahjoub et al., 2004). The kinase activity of Fa2p was also found to be necessary for microtubule severing to occur during deflagellation.

Attempts to identify the ADF1 gene using the insertional mutants generated in the genetic screen revealed that the insertional marker segregated away from the *adf1* phenotype (Finst et al., 1998). Since the *adf1* mutant can deflagellate when calcium influx, activated by low pH, is bypassed (by the addition of detergent) it must play a role in the calcium-signalling pathway during deflagellation. Calcium influx assays reveal that *adf1* mutants have no calcium influx when treated with acid (Quarmby and Hartzell, 1994; Wheeler et al., 2008). This suggests that the ADF1 gene could encode a pH sensitive ion channel or a protein involved in the activation of the channel. Further support for this theory comes from the ability to block calcium influx and thus deflagellation with known calcium channel blockers (Quarmby and Hartzell, 1994; Quarmby, 1996). Both lanthanum (La^{3+}) and Gadolinium (Gd^{3+}) block calcium influx and acid induced deflagellation in WT

cells. The following chapter tells the story of how a previous graduate student Jaime Kirschner mapped ADF1, and how she and I attempted (and failed) to identify the ADF1 gene.

Though the genetic screen was saturated, multiple alleles for all three genes were found through insertional and UV mutagenesis, only three genes were identified. However, no microtubule severing or calcium sensing proteins, which we know must be involved in deflagellation, were recovered in the screen. It is our hypothesis that these genes also play important roles in the severing seen during pre-mitotic reabsorption and are thus essential for the cell. If this is the case then null mutations in these genes would be lethal and these mutants would never be recovered. Conversely, other proteins that normally work together with them could compensate mutations in these genes, masking the mutant phenotype. In either case these null mutants would not be recovered. Chapter 3 describes a new deflagellation genetic screen designed to overcome this problem. It also describes my mapping of one of the new genes discovered in this screen.

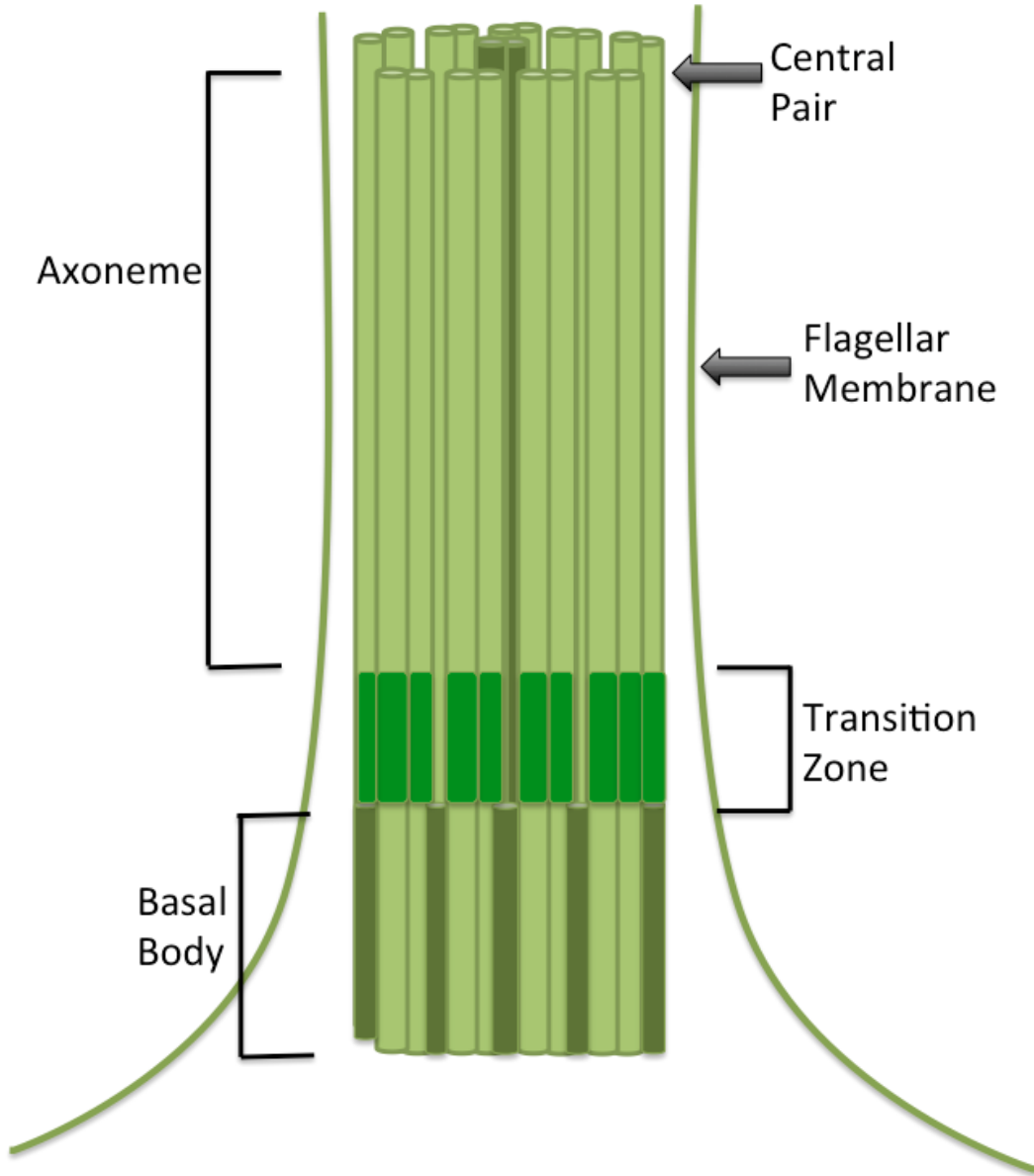
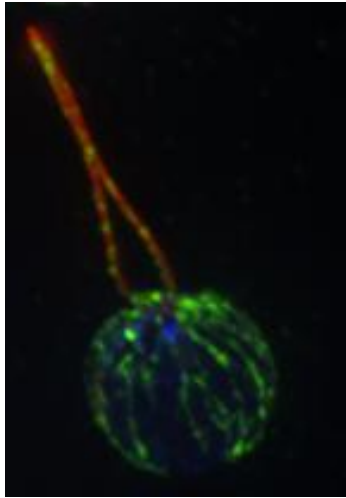


Figure 1-1: Schematic of a typical motile cilium (flagellum).

The diagram shows the microtubule arrangement of a cilium or flagellum. The basal body is a specialized centriole composed of nine triplet microtubules. The transition zone is where the basal body triplet microtubules are exchanged for doublet microtubules that make up the cilium proper; it also functions as a gate restricting access to the flagellum. The core of the cilium is the axoneme. In the motile cilium seen here the axoneme encases a central pair of microtubules. The axoneme grows from the ciliary tip (plus end of the microtubules) and it's at the tip where antereograde and retrograde motors are switched.

A



B

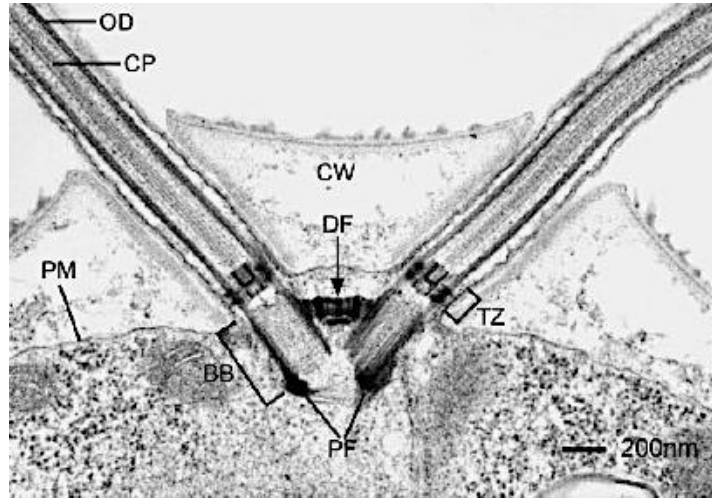


Figure 1-2: The model organism *Chlamydomonas reinhardtii* and its two flagella.

(A) An immunofluorescence image of *Chlamydomonas* depicting the cell body (green- α & β tubulin), flagella (red- acetylated tubulin), a basal body protein (blue-Centrin) and a ciliary protein (yellow- CNK2). Image by Laura Hilton, unpublished. (B) Scanning electron micrograph of *Chlamydomonas* flagella and basal bodies. In *Chlamydomonas* the transition zone forms an electron dense H-structure. CW: cell wall; PM: plasma membrane; OD: outer doublets of axoneme; CP: central pair microtubules; TZ: transition zone; BB: basal bodies; DF: distal striated fiber; PF: proximal fiber connecting basal bodies. Micrograph by Dr. William Dentler published in Silflow & Lefebvre, 2001. Copyright by the American Society of Plant Biologists, reprinted with permission.

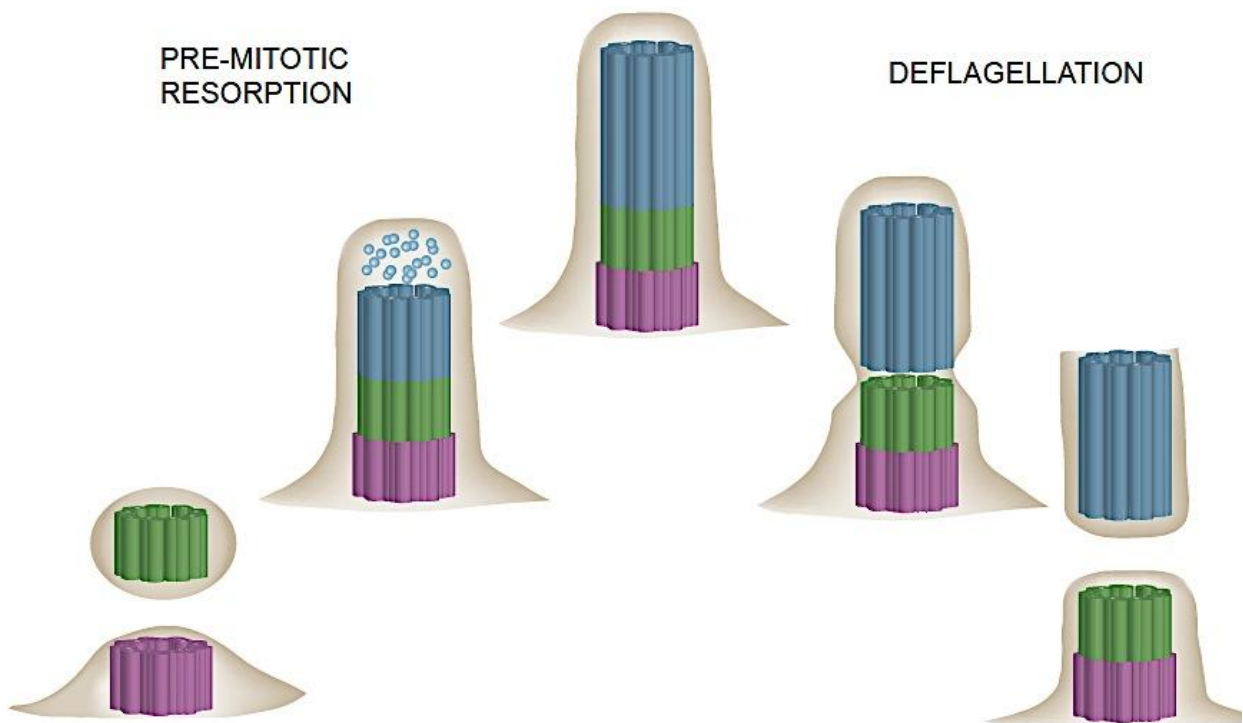


Figure 1-3: Schematic comparing the two modes of ciliary disassembly.

Prior to cell division cilia are reabsorbed back into the cell. This occurs by removing the flagellar components from the tip. It has been shown that after the flagella are reabsorbed there is a severing event proximal to the transition zone releasing the transition zone and allowing the basal bodies to participate in mitosis (Parker et al., 2010). In deflagellation the axoneme and flagellar membrane are severed at a site distal to the transition zone resulting in the shedding of the flagellum. This mechanism occurs in response to a physical or chemical stress signal, which is calcium dependent. Image by Laura Hilton, unpublished.

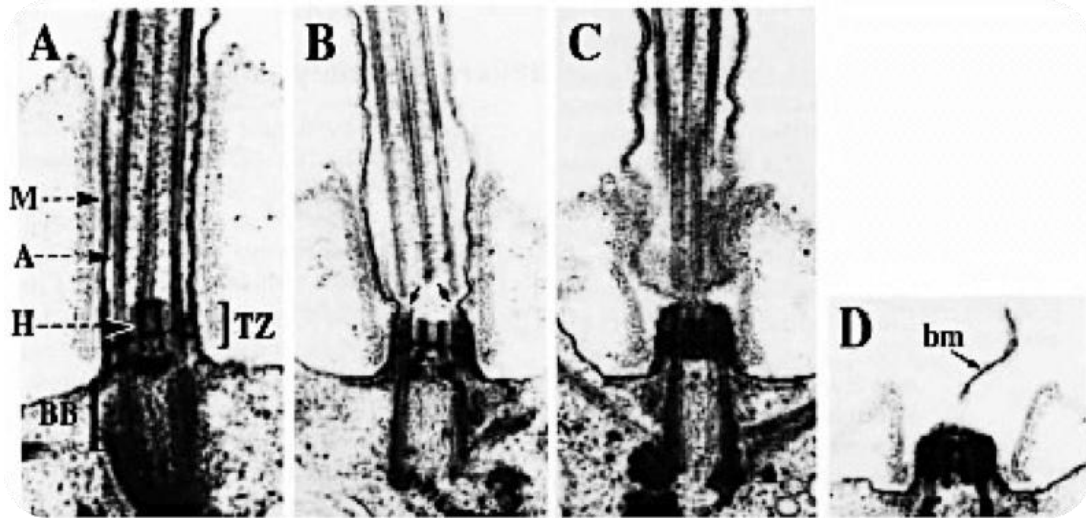


Figure 1-4: Transmission electron micrographs of deflagellation in *Chlamydomonas*.

Flagellar autotomy (or deflagellation) occurs by: the severing of the nine outer doublets of the axoneme and the pinching off of the flagellar membrane, resulting in the shedding of the flagellum (A-D). Severing occurs distal to the transition zone, thus, the transition zone remains with the cell. M: membrane; A: axoneme; TZ: transition zone, in *Chlamydomonas* it forms an H-structure (H); BB: basal body; BM: X. Micrographs by Lewin & Lee, 1985.

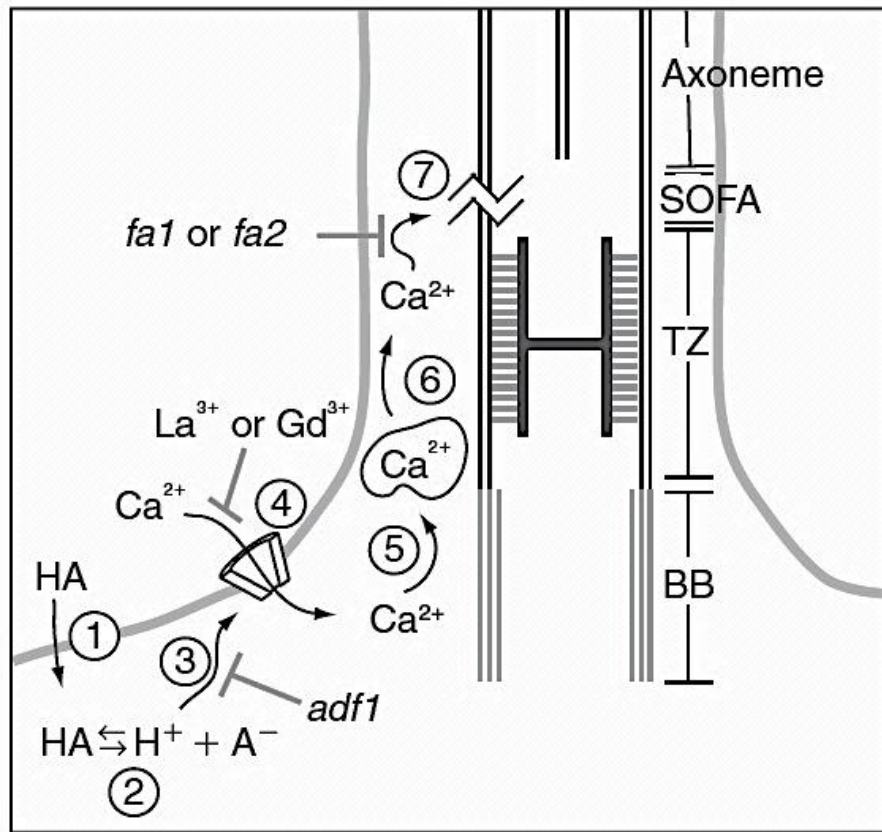


Figure 1-5: Schematic diagram of the signalling pathway for acid-induced deflagellation.

(1) Protonated forms of weak acids permeate the cell membrane. (2) In the cytosol the weak acid dissociates causing intracellular acidification. (3) Acidification results in the activation of a calcium-influx pathway. The *adf1* mutants are defective in this calcium influx step. (4) Calcium influx is blocked by lanthanum and gadolinium. (5) The extracellular calcium then activates the release of calcium from an intracellular store yet to be identified. (6) This intracellular calcium, through a calcium-sensing protein, activates the microtubule severing machinery. The outer doublets are severed at the SOFA, site of flagellar autotomy, distal to the transition zone. The *fa* mutants are blocked at the severing step. Both FA1 and FA2 localize to the SOFA. ADF1 is yet to be identified. BB: basal body; TZ: transition zone. Quarmby, 2009. Copyright by Elsevier, reprinted with permission.

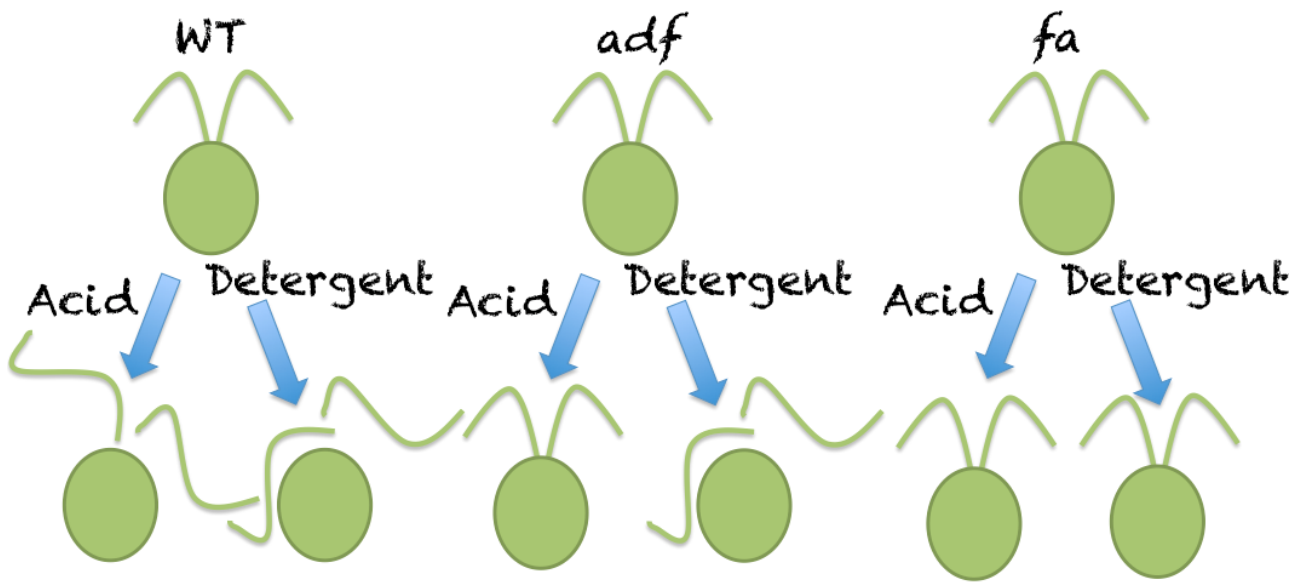


Figure 1-6: The deflagellation mutant phenotypes.

Schematic depicting the two acid-induced deflagellation mutant phenotypes: *adf* and *fa*. For both mutants weak organic acids fail to induce deflagellation. When they are placed in detergent, allowing calcium influx by bypassing the signalling pathway, the *adf* mutants are able to deflagellate indicating that they are deficient in this calcium signalling. The *fa* mutants, however, retain their flagella suggesting that they are deficient in the activation of the severing machinery. Calcium influx assays further support this as no calcium influx is seen in the *adf* mutants but is present in the *fa* mutants.

Allele	Description
<i>adf1-1</i>	Unlinked mutation in <i>imp4</i>
<i>adf1-2</i>	Insertional mutagenesis
<i>adf1-3</i>	Insertional mutagenesis
<i>adf1-4</i>	Insertional mutagenesis
<i>adf1-5</i>	Insertional mutagenesis
<i>adf1-6</i>	UV mutagenesis
<i>fa1-1</i>	Previously <i>fa1</i>
<i>fa1-2</i>	Insertional mutagenesis
<i>fa1-3</i>	Insertional mutagenesis
<i>fa1-4</i>	Insertional mutagenesis
<i>fa1-5</i>	UV mutagenesis
<i>fa2-1</i>	Insertional mutagenesis
<i>fa2-2</i>	UV mutagenesis
<i>fa2-3</i>	Insertional mutagenesis
<i>fa2-4</i>	Insertional mutagenesis

Table 1-1: The Deflagellation mutants identified in the 1998 genetic screen

The Finst et al., 1998 genetic screen recovered five new alleles of the previously identified *adf1-1* mutant, four alleles of the previously identified *fa1-1* mutant, and four alleles of a novel mutant *fa2*. FA1 is a predicted scaffolding protein located on chromosome 6, while FA2 is a NIMA-related kinase (NEK) that maps to chromosome 7. Both FA1 and FA2 localize to the SOFA. The ADF1 gene has yet to be identified, but has been mapped to a 350kb region on chromosome 9.

References

- Antenedo C, Rodahl AM, Miering E, Heynen ML, Senisterra GA, Lepock JR: Interaction of dibucaine with the transmembrane domain of the Ca²⁺-ATPase of sarcoplasmic reticulum. *Biochemistry* 33: 12283-12290, 1994
- Badu D, Roy S: Left-right asymmetry: cilia stir up new surprises in the node. *Open Biol* 3: doi: 10.1098, 2013
- Berbari NF, Pasek RC, Malarkey EB, Yazdi SM, McNair AD, Lewis WR, Nagy TR, Kesterson RA, Yoder BK: Leptin resistance is a secondary consequence of the obesity in ciliopathy mutant mice. *Proc Natl Acad Sci USA* 110: 7796-7801, 2013
- Blum JJ: Existence of a breaking point in cilia and flagella. *J Theor Biol* 33: 257-263, 1971
- Casano C, Roccheri MC, Maenza L, Migliore S, Gianguzza F: Sea urchin deciliation induces thermoresistance and activates the p38 mitogen-activated protein kinase pathway. *Cell Stress Chaperones* 8: 70-75, 2003
- Catterall WA: Cellular and molecular biology of voltage-gated sodium channels. *Physiol Rev* 72: S15-S48, 1992
- Cavalier-Smith T: Basal body and flagellar development during the vegetative cell cycle and the sexual cycle of *Chlamydomonas reinhardtii*. *J Cell Sci* 16: 529-556, 1974
- Christensen ST, Pendersen LB, Schneider L, Satir P: Sensory cilia and integration of signal transduction in human health and disease. *Traffic* 8: 97-109, 2007.
- Dymek EE, Smith EF: PF19 encodes the p60 catalytic subunit of katanin and is required for assembly of the flagellar central apparatus in *Chlamydomonas*. *J Cell Science* 125: 3357-3366, 2012

- Estrada-Cuzcano A, Roepman R, Cremers FPM, den Hollander AI, Mans DA: Non-syndromic retinal ciliopathies: translating gene discovery into therapy. *Human Molecular Genetics* 21: R111-R124, 2012
- Evans JH, Smith JL, Keller LR: Ion selectivity in the *Chlamydomonas reinhardtii* flagellar regeneration system. *Exp Cell Res* 230: 94-102, 1997
- Finst RJ, Kim PJ, Quarmby LM: Genetics of the Deflagellation Pathway in *Chlamydomonas*. *Genetics* 149: 927-936, 1998
- Finst RJ, Kim PJ, Griffis ER, Quarmby LM: Fa1p is a 171kDa protein essential for axonemal microtubule severing in *Chlamydomonas*. *J Cell Science* 113: 1963-1971, 2000
- Friedrich RW, Korsching SI: Combinatorial and chemotopic odorant coding in the zebrafish olfactory bulb visualized by optical imaging. *Neuron* 18: 737-752, 1997
- Hilderbrandt F, Benzing T, Katsanis N: Ciliopathies. *N Engl J Med* 364: 1533-1543, 2011
- Inglis PN, Borojevich KA, Leroux MR: Piecing together a ciliome. *Trends Genet* 22: 491-500, 2006
- James TY, Kauff F, Schoch CL, Matheny PB, Hofstetter V, Cox CJ, Celio G, Gueidan C, Fraker E, Miadlikowska J: Reconstructing the early evolution of Fungi using a six-gene phylogeny. *Nature* 443: 818-822, 2006
- Kim JI, Kim J, Jang HS, Noh MR, Lipschutz JH, Park KM: Reduction of oxidative stress during recovery accelerates normalization of primary cilia length that is altered after ischemic injury in murine kidneys. *Am J Physiol Renal Physiol* 304: F1283-F1294, 2013
- Kishimoto N, Sawamoto K: Planar polarity of ependymal cilia. *Differentiation* 83: S86-S90, 2012
- Ko JY, Park JH: Mouse models of polycystic kidney disease induced by defects of ciliary proteins. *BMB Rep* 46: 73-79, 2013

- Kotsis F, Boehlke C, Kuehn EW: The ciliary flow sensor and polycystic kidney disease. *Nephrol Dial Transplant* 28: 518-526, 2013
- Kuin H, Koerten H, Ghijsen WE, Munnik T, van den Ende H, Musgrave A: Chlamydomonas contains calcium stores that are mobilized when phospholipase C is activated. *Planta* 210: 268-294, 2000
- Lewin RA, Lee TH, Fang LS: Effects of various agents on flagellar activity, flagellar autotomy and cell viability in four species of Chlamydomonas (Chlorophyta: Volvocales). In: *Prokaryotic and Eukaryotic Flagella* (Amos WB, Duckett JG, Eds.) *Soc Exp Biol Symp* 35: 421-437, 1982
- Lewin RA and Burrascano C: Another new kind of Chlamydomonas mutant, with impaired flagellar autotomy. *Experientia* 39: 1397-1398, 1983
- Lewin RA, Lee KW: Autotomy of algal flagella: electron microscope studies of Chlamydomonas (Chlorophyceae) and Tetraselmis (Prasinophyceae). *Phycologia* 24: 311-316, 1985
- Lienkamp S, Ganner A, Walz G: Inversin, Wnt signalling and primary cilia. *Differentiation* 83: S49-S55, 2012
- Lohret TA, McNally FJ, Quarmby LM: A role for katanin mediated axonemal severing during Chlamydomonas severing. *Mol Biol Cell* 9: 421-437, 1998
- Lohret TA, Zhao L, Quarmby LM: Cloning of Chlamydomonas p60 Katanin and localization to the site of outer doublet severing during deflagellation. *Cell Motil Cytoskeleton* 43: 221-231, 1999
- Mahjoub MR, Montpetit B, Zhao L, Finst RJ, Goh B, Kim AC, Quarmby LM: The fa2 gene of Chlamydomonas encodes a NIMA family kinase with roles in cell cycle progression and microtubule severing during deflagellation. *J Cell Science* 115: 1759-1768, 2002
- Mahjoub MR, Rasi MQ, Quarmby LM: A NIMA-related kinase, Fa2p, localizes to a novel site in the proximal cilia of Chlamydomonas and mouse kidney cells. *Mol Biol Cell* 15: 5172-5186, 2004
- Maier JX, Wachowiak M, Katz DB: Chemosensory convergence on primary olfactory cortex. *J Neuroscience* 32: 17037-17047, 2012

- Manning DK, Sergeev M, van Heesbeen RG, Wong MD, Oh JH, Liu Y, Henkelman RM, Drummond I, Shah JV, Beier DR: Loss of the ciliary kinase Nek8 causes left-right asymmetry defects. *J Am Soc Nephrol* 24: 100-112, 2013
- Marshall WF, Rosenbaum JL: Intraflagellar transport balances continuous turnover of outer doublet microtubules: implications for flagellar length control. *J Cell Biol* 155: 405-414, 2001
- McNally KP, Barzirgan OA, McNally FJ: Two domains of p80 katanin regulate microtubule severing and spindle pole targeting by p60 katanin. *J Cell Sci* 113: 1623-1633, 2000
- Mohammed BJ, Mitchell TJ, Andrew PW, Hirst RA, O'Callaghan C: The effect of pneumococcal toxin, pneumolysin, on brain ependymal cilia. *Microb Pathog* 27: 303-309, 1999
- Mukhopadhyay S, Jackson PK: The tubby family proteins. *Genome Biol* 12: doi: 10.1186, 2011
- Mukhopadhyay S, Wen X, Ratti N, Loktev A, Rangell L, Scales SJ, Jackson PK: The ciliary G-protein-coupled receptor Gpr161 negatively regulates the Sonic hedgehog pathway via cAMP signalling. *Cell* 152: 210-223, 2013
- Parker JDK, Hilton LK, Diener DR, Rasi MQ, Mahjoub MR, Rosenbaum JL, Quarmby LM: Centrioles are freed from cilia by severing prior to mitosis. *Cytoskeleton* 67: 425-430, 2010
- Pickett-Heaps J, Pickett-Heaps J: *Predatory Tactics: Survival in the Microcosmos*. NTSC videocassette, 42 minutes. Cytographics, Ascot Vale, Australia. 1996
- Pier B, Kazanjian A, Gillette L, Strengen K, Burney RO: Effect of cigarette smoking on human oviductal ciliation and ciliogenesis. *Fertil Steril* 99: 199-205, 2013
- Quader H, Chrniack J, Filner P: Participation of calcium in flagellar shortening and regeneration in *Chlamydomonas reinhardtii*. *Exp Cell Res* 113: 295-301, 1978
- Quarmby LM: Ca²⁺ influx activated by low pH in *Chlamydomonas*. *J Gen Physiol* 108: 351-361, 1996

- Quarmby LM: Cellular deflagellation. *Int Rev cytol: Suv Cell Biol* 233: 47-91, 2004
- Quarmby LM: Deflagellation. In: *The Chlamydomonas Sourcebook, Cell Motility and Behavior* (Witman G, Ed) 3:43-69, 2009
- Quarmby LM, Yueh YG, Cheschire JL, Keller LR, Snell WJ, Crain RC: Inositol phospholipid metabolism may trigger flagellar excision in *Chlamydomonas reinhardtii*. *J Cell Biol* 116: 737-744, 1992
- Quarmby LM, Hartzell HC: Two distinct, calcium-mediated, signal transduction pathways can trigger deflagellation in *Chlamydomonas reinhardtii*. *J Cell Biol* 124: 807-815, 1994
- Quarmby LM, Parker JDK: Cilia and the cell cycle? *J Cell Biol* 169: 707-710, 2005
- Rasi MQ, Parker JDK, Feldman JL, Marshall WF, Quarmby LM: Katanin knockdown supports a role for microtubule severing in release of basal bodies before mitosis in *Chlamydomonas*. *Molec Biol Cell* 20: 379-388, 2009
- Roll-Mecak A, McNally FJ: Microtubule severing enzymes. *Curr Opin Cell Biol* 22: 96-103, 2010
- Rosenbaum JL, Child FM: Flagellar regeneration in protozoan flagellates. *J Cell Biol* 34: 345-364, 1967
- Silflow CD, Lefebvre PA: Assembly and motility of eukaryotic cilia and flagella. Lessons from *Chlamydomonas reinhardtii*. *Plant Physiol*: 127: 1500-1507, 2001
- Sanders MA, Salisbury JL: Centrin plays an essential role in microtubule severing during flagellar excision in *Chlamydomonas reinhardtii*. *J Cell Biol* 124: 795-805, 1994
- Tadenev AL, Kulaga HM, May-Simera HL, Kelley MW, Ksanis N, Reed RR: Loss of Bardet-Biedl syndrome protein-8 (BBS8) perturbs olfactory function, protein localization, and axon targeting. *Proc Natl Acad Sci USA* 108: 10320-10325, 2011

Veland IR, Montjean R, Eley L, Pendersen LB, Schwab A, Goodship J, Kristiansen K, Pendersen SF, Saunier S, Christensen ST: Inversin/Nephrocystin-2 is required for fibroblast polarity and directional cell migration. *Plos One* 8(4): e60193, 2013

Wang Y, Nathans J: Tissue/planar cell polarity in vertebrates: new insights and new questions. *Development* 134: 647-658, 2007.

Wheatley DN: Primary cilia in normal and pathological tissues. *Pathobiology* 63: 222-238, 1995

Wheatley DN, Wang AM, Strugnell GE: Expression of primary cilia in mammalian cells. *Cell Biol Int* 20: 73-81, 1996

Wheeler GL, Joint I, Brownlee C: Rapid spatiotemporal patterning of cytosolic Ca²⁺ underlies flagellar excision in *Chlamydomonas reinhardtii*. *Plant J* 53: 401-413, 2008

Wickstead B, Gull K: Dyneins across eukaryotes: a comparative genomic analysis. *Traffic* 8: 1708-1721, 2007

Willaredt MA, Gorgas K, Gardner HA, Tucker KL: Multiple essential roles for primary cilia in heart development. *Cilia* 1: 23, 2012

Wilson NF, Iver JK, Buchheim JA, Meek W: Regulation of flagellar length in *Chlamydomonas*. *Semin Cell Dev Biol* 19: 494-501, 2008

2. ADF1: The acid deflagellation gene 1

2.1 Linkage analysis map of ADF1

The 1998 genetic screen generated four *adf1* mutant alleles through insertional mutagenesis (Finst el al., 1998). When attempts were performed to identify the ADF1 gene with these alleles it was discovered that the *adf1* mutation was unlinked to the insertional marker. This could be due to the marker having been excised from the gene by the cell, possibly creating a deletion in the process, or that these *adf1* mutants are spontaneous deflagellation mutants identified in the screen. In order to identify the ADF1 gene linkage analysis was performed using PCR-based recombination frequency mapping. This approach analyzes the recombination frequency between a genetic marker, in this case the *adf1* deflagellation phenotype, and a molecular marker, with known chromosomal coordinates. Using this method Jeremy Parker, a previous grad student in the Quarmby lab, mapped ADF1 to a 2.3Mb region between the molecular markers Oee1 and V1Sc101 on linkage group IX (Jeremy Parker, unpublished data). With this initial linkage data Jaime Kirschner, another previous graduate student, narrowed the ADF1 gene locus to ~380kb (Kirschner, 2009).

The PCR-based recombination frequency mapping approach requires the analysis of a large number of progeny from crosses between the *adf1* mutant and a polymorphic mapping strain. *Chlamydomonas* can reproduce both sexually and asexually (Figure 2-1). Sexual crosses between the mutant strains and a polymorphic strain, used for genetic mapping, were performed by first inducing gametogenesis in the individual strains. This is

accomplished by growing the strains on low nitrogen media. The strains, with opposite mating types (plus and minus), are then mixed allowing for mating type plus cells to fuse with mating type minus. Following zygote formation a protective wall is made which encases the zygote guarding it from the environment. The zygotes are then incubated in the dark, where they develop, and when they are next exposed to the light (at least three days later) they undergo germination. Tetrad progeny (zoospores) can then be recovered for genetic analysis.

To efficiently identify recombinant progeny strains for PCR analysis, Jaime first created an *adf1* double mutant with *pf16*, a mutant located on the same arm as *adf1* on linkage group IX. This double mutant she then crossed with the polymorphic mapping strain, S1D2, and analyzed only the single mutant progeny, since a recombination event between *adf1* and *pf16* had to have occurred in these strains. These recombination events in the single mutants, that separated the two mutations, would thus allow her to determine the boundary separating the ADF1 locus from *pf16*. The genomic DNA from the single mutants were then extracted and prepared for PCR. For these PCR reactions Jaime created her own molecular markers, as there were few previously made markers in the ADF1 region. To make these markers she amplified 2kb introns from predicted genes in the region and performed restriction digests. Digests that generated differences in banding patterns between the parental controls (*adf1/pf16* and S1D2) were used for linkage analysis. Despite her efforts the ADF1 region contains few polymorphisms that could be used to generate molecular markers, thus only a small quantity of introns were used as molecular markers for her linkage analysis.

Looking at 75 single mutant tetrad progeny, Jaime was able to map ADF1 to a ~380kb region using PCR-based recombination frequency mapping (Figure 2-2). The mapping proved particularly difficult due to the lack of molecular markers, as stated above,

and because of the low recombination frequency observed (4%). The region, located on chromosome 9: 4576290-4957883 on the current genome browser (www.phytozome.net), is located left of a predicted centromere, between the molecular markers Oee1/171503b and 169190. The ADF1 locus can be broken down into three sections: (1) a 280kb region, (2) a ~40kb region (3) a ~50kb region (Figure 2-3). The 280kb region, located on chromosome 9: 4576290-4867854, contains 40 predicted genes in the annotated genome browser that are spanned by ten BACs. The ~40kb region, on chromosome 9: 4867855-4907332, has five gene predictions which are not covered by any BACs. The ~50kb region, on chromosome 9:4907333-4957883, is a sequence gap in the genome with no annotations. Although the entire *Chlamydomonas* genome has been sequenced and annotated sequence gaps remain. These gaps are found near predicted centromeres, like in the case of the ~50kb gap in the ADF1 gene locus, and presumably arise from difficulties in sequencing due to high GC content (*Chlamydomonas* is 65% GC rich) and the presence of highly repetitive sequences.

Following her mapping Jaime attempted to identify the ADF1 gene by performing phenotypic rescue assays with predicted genes in the 280kb sub-region. The assays were performed by co-transforming *adf1* mutant cells with linearized BAC DNA and a selectable marker that conferred resistance to the antibiotic Pararomycin (PAR). The transformed cells were then plated on media containing PAR and the resulting colonies were individually screened for deflagellation. Though Jaime screened hundreds of colonies transformed with the various BACs she was unable to recover a rescue of the *adf1* mutant.

2.2 Rescuing ADF1

I began my Master's by continuing where Jaime left off in the attempts to rescue *adf1*, the results of which are told in this section. I had two main resources to test for ADF1: (1) the BACs from the 280kb region of the ADF1 locus, and (2) sub-clones of the five predicted genes from the ~40kb region. Though Jaime had already assayed hundreds of colonies transformed with BAC DNA from the 280kb region, the numbers still remained low for many of the gene predictions due to low transformation efficiency of BAC DNA. My objective was to perform more rescue assays for all of the gene predictions in the ADF1 region, thereby increasing the chances of identifying ADF1. If no rescue was obtained with these predictions then my work would help rule out ADF1 from being in the 280kb and 40kb regions, and we would have to find ways to characterize the ~50kb sequence gap. For the five gene predictions in the 40kb sub-region (39-43), the genes corresponding to the predictions were sub-cloned into the pSI103 vector, which contained the selectable marker PAR. This was done by Ziwei Ding from the Molecular Biology Service Center and by Adam Staniscia, an undergrad in the lab.

Early into the rescue assays I obtained a rescue of the *adf1-3* mutant allele with BAC24114 (Figure 2-4). This BAC had been linearized with EcoRI creating six BAC fragments prior to transformation (Figure 2-5). To test whether this was a rescue, a WT contaminant or a spontaneous reversion I backcrossed the rescue strain with a WT strain and assayed for the deflagellation phenotype of the progeny. If this was: (A) a WT contaminant or reversion then all of the progeny would be WT for deflagellation, but if this was (B) a rescue then a quarter of the progeny should exhibit the *adf1* phenotype. Consistent with my prediction, of 56 random progeny assayed 18 (32%) were *adf* for deflagellation. Thus, it appeared that I had succeeded in the first step of my Master's goal by rescuing *adf1-3*! No rescue was obtained with any other BAC or sub-clone.

BAC24I14 contains fifteen full gene predictions and half of a predicted 40kb ATM/ATR-related phosphatidylinositol 3-kinase (gene prediction g.9861.t1 or 28). Of interest to us was the g9856.t1 gene prediction (gene prediction 22), which is a predicted transient receptor/potential ion channel protein. ADF1 is part of a pathway that contains an ion channel that when activated by low pH allows for the influx of extracellular calcium, the channel was therefore a good candidate. Other gene predictions on BAC24I14 were also of interest. These include g9848.t1 (14), which is predicted to be a GTPASE-Activating protein and g9852.t1 (18), a cytochrome p450.

My next steps were to confirm the rescue and identify the ADF1 gene. Having only screened 395 colonies transformed with BAC24I14 to obtain the first rescue (#341) I expected to only have to screen a few hundred colonies more to generate a second *adf1* rescue. This proved, however, to not be the case. I screened a further 2093 colonies transformed with BAC 24I14, either digested with EcoRI or other restriction enzymes (Ascl, BstBI, ClaI, and XhoI) or undigested BAC, but was unable to recover a second *adf1* rescue. Additional transformations were also done with BAC1F13, BAC16D2 and BAC34H14 (816 colonies), which cover genes present in BAC24I14 (Figure 2-3). No *adf1* rescue was obtained with any of these BACs.

At the same time that I was trying to acquire a second rescue I was also attempting to identify if, and which, fragment of BAC24I14 was responsible for rescuing the phenotype in *adf1-3*. If a fragment of BAC24I14 was associated with the rescue then a second copy of this fragment (from BAC24I14) should be present in the genome of the *adf1-3* rescue strain. My approach was then to create radioactively labeled probes for genes present in the six BAC fragments and search for an extra insertion site in the *adf1-3* rescue strain. Prior to doing the experiment I crossed the rescue strain to *adf1-1* and recovered a progeny strain (N1) that was WT for deflagellation. This cross was done to reduce extra

insertions of BAC DNA or selectable marker (50% of unlinked insertions will be removed with a single out cross) that were not associated with the rescue event.

Having performed the backcross, I used Southern blots to determine which part of BAC24114 inserted into the genome of the N1 progeny strain. The genomic DNA of N1 was extracted, digested, separated by gel electrophoresis and then transferred to a positively charged nylon membrane for probe hybridization. The probes were made using the Bca polymerase from Takara (Mountain View, USA). I first amplified the DNA for the probes from BAC DNA, via PCR, and then gel extracted the PCR products. These were then incubated with the polymerase, dNTPs (A, G and T) and [α - 32 P] dCTP for 3 hours; the unincorporated dCTP was then removed using a column extraction PCR purification protocol. The nylon membranes were pre-hybridized in hybridization buffer for 2 hours at 37°C and the purified probe was then added with fresh buffer and incubated overnight. Four washes were performed the next day to remove unbound probe. Following washes the membranes were exposed to film for ~18hours for probe detection.

The southern blot films for two of the probes are seen in Figure 2-6. For probe 1 the gene prediction # 13 was originally fully inside the second BAC fragment (in v4 of the genome browser) when I created the probe and performed the southern blot. This prediction has now been shifted to the right and only the 5'UTR, the first exon and part of the first intron remain in this fragment of BAC24114. For both southern a parental *adf1* control was performed to compare the banding pattern of the N1 strain (R in Figure 2-6). No extra insertion/copy was observed for probes 1 and 2.

As the numbers of colonies continued to climb without a second rescue I started to suspect the veracity of the rescue. To test the possibility that I had created a suppressor, I further examined the progeny of the *adf1-1* x *adf1-3* rescue cross. If I had indeed rescued *adf1-3* with a second site insertion of the ADF1 gene, then I would expect 50% of the

progeny strains to be WT for deflagellation and the other 50% to exhibit the *adf* phenotype. Consistent with this, 64 of the 115 random progeny screened (56%) were WT for deflagellation. What surprised me was that a 100% of the WT strains retained the PAR selectable marker while none of the *adf1* progeny did (this was confirmed by PCR and growing the strains on media with PAR), indicating that PAR is tightly linked to the component responsible for the WT rescuing phenotype. So given that: (1) no second rescue was obtained with BAC24I14, and that (2) the selectable marker co-segregates 100% with the rescuing phenotype- it is my hypothesis that a suppressor of *adf1-3* was generated in the attempts to rescue the *adf* phenotype. In *Chlamydomonas* exogenous DNA during nuclear transformations inserts into the genome randomly through non-homologous recombination. It is therefore possible that the PAR marker was inserted in a novel gene that when disrupted allows for deflagellation to occur normally in response to acid.

It is also possible that the reason why the PAR marker co-segregates with the WT deflagellation phenotype is because it was inserted into the genome in close vicinity of a fragment from BAC24I14, allowing for the observed retention of the marker in the backcrossed progeny. If this is the case then it is still possible that the ADF1 gene is present in BAC24I14. Despite having assayed >2000 colonies transformed with BAC24I14, there is a possibility that these transformants did not contain the fragment in which ADF1 is on. Since transformants are only selected based on the PAR insertion, this is a likely scenario. As a first step in determining whether the PAR marker had inserted and thus disrupted a novel gene, or was linked to a fragment of BAC24I14 I attempted to identify the PAR insertion site.

2.3 The Search for PAR

To identify where in the genome the PAR selectable marker was inserted I began by performing a PAR southern blot. As was done with the previous southern blots the genomic DNA from the N1 progeny strain was extracted, digested, separated by gel electrophoresis then transferred to a nylon membrane for probe hybridization. The template DNA for the PAR probe was amplified by PCR from the vector used in the transformations, pSI103, then gel extracted. The purified PCR product was then incubated at room temperature with *E. coli* Klenow fragment and dNTPs (A, G, T and [α -³²P] dCTP). As done with the previous probes, unincorporated isotope was removed using a column extraction PCR purification protocol. The probe was then hybridized as before.

Digesting the genome of the N1 strain with HindIII and SmaI (individually) generated a ~7.5kb and ~6.5kb PAR insertion sites (Figure 2-7, S2-1). Two WT strains (137c+ and 137c-) were used as negative controls, since they don't contain the PAR marker, while pSI103 (the vector containing the PAR marker) was used as a positive control. My next goal was to identify the DNA flanking the PAR marker. To achieve this four approaches were taken: (1) Self-ligation PCR, (2) TAIL-Adaptor PCR, (3) Colony lifts and (4) Linkage mapping. However, I was unable to get any of these to work, but for the record these approaches are described in the remaining pages of this section.

For the first method, Self-ligation PCR, the bands containing the PAR insertion sites were extracted and a ligation reaction was performed so that the ends could ligate unto themselves. The reaction was then digested with an enzyme that cuts inside the selectable marker thereby re-linearizing the band (Figure 2-8). PCR was then performed using primers that annealed to either end of the digested PAR marker, thus, the PCR would only work if the marker ends remain attached to the same piece of DNA (i.e. the

enzyme does not digest the flanking DNA). With this approach I was able to amplify a ~3kb band from the 6.5kb *Sma*I insertion site (Figure 2-9A). A ~700bp band was also amplified but this band I concluded to be non-specific because I also generated it when PCR was done on the *adf1* control, which does not contain the PAR marker. Following optimization of the PCR, so that only the 3kb product was amplified, the product was gel extracted, ligated into pGEMT and transformed into chemically competent *Escherichia coli* (*E.coli*). The transformed bacteria were then plated on selective media and plasmid extractions performed on the resulting colonies. PCR and restriction digest was used to identify positive constructs (Figure 2-9B, C). These positive constructs were then sent for sequencing.

Sequencing of this 3kb band revealed that there was a fragment of BAC24I14 beside the PAR marker (S2-2), which contained a predicted cytochrome p450. Unfortunately, I realized that I had performed this method on the original *adf1-3* rescue strain only and not the backcrossed N1 progeny (used to identify the PAR insertion sites). However, when the method was applied to the N1 strain the 3kb product was not generated (Figure 2-9D). Several attempts to reproduce the 3kb in N1 were performed but all were unsuccessful leading me to conclude that this fragment of BAC24I14 was no longer present in the out backcrossed progeny, and thus, not involved in the rescuing of the *adf1-3* strain.

It is my hypothesis that the 3kb band indicates that there was an extra PAR and BAC DNA insertion site that was subsequently removed when the original *adf1-3* rescue strain was crossed to *adf1-1*. Since in order to obtain the PAR insertion sites I extracted DNA ± 0.5 kb from the expected insertion bands from whole genome digest (i.e. for the 6.5kb *Sma*I band I extracted DNA from 6-7kb) this extra insertion site must have extracted along. Because I was unable to amplify the flanking DNA from either of the PAR insertion

sites in the N1 strain using Self-ligation PCR I decided to try the TAIL-Adaptor PCR approach. This method I hoped would allow me to more specifically target the bands containing the PAR insertion sites.

In TAIL-Adaptor PCR (Iomini et al., 2009), the bands containing the insertion sites were gel extracted from whole genome digests and digested again to generate blunt ends (Figure 2-10). DNA adaptors were then ligated to the ends and PCR was performed with primers specific for PAR and the adaptors. Using this method I was able to amplify a ~1.3kb band from the 6.5kb *Sma*I PAR insertion site (Figure 2-11). Several attempts were made to sub-clone this band into pGEMT for sequencing but I was unsuccessful. It appeared that I had sub-cloned the band once, but sequencing yielded only vector sequence (S2-2). The 1.3kb band was also sent in for sequencing without being sub-cloned but no sequence was generated. This method was performed several times, varying the restriction enzyme used to produce the blunt-ends, but I was unable to amplify anything from these constructs.

The third approach I used was colony lifts, where the insertion site bands were sub-cloned into pGEMT and transformed into bacteria (Figure 2-12). I had originally thought to screen the colonies for positive transformants through Blue/White selection but realized that colony lifts would be a more efficient way to screen for the presence of the PAR bands in the transformants. Therefore, the colonies were transferred onto a colony lift membrane and their DNA was released and fixed. I used the same PAR probe used to find the PAR insertion sites to probe the colony lift membranes. Like with the southern blots the membranes were first pre-hybridized in buffer, the probe was then added and incubated overnight and the membranes washed then exposed to film for ~18 hours.

A positive vector control was performed on the colony lift protocol where pSI103 was diluted and transformed into chemically competent Mach1 *E.coli* cells along with

pBlueScript (Figure 2-13A). Though the transfer was smeary, only a few colonies exhibited strong PAR signal consistent with the small amount of pSI103 used. Colonies transformed with the constructs that displayed a strong signal with the PAR probe were grown separately and plasmid extractions were performed on them (Figure 2-13B, C). PCR for the PAR marker was then performed on the plasmids to identify those containing the PAR insertion sites. Despite displaying strong PAR signal in the colony lifts all the plasmids that were further analyzed were found to be negative in the PAR PCRs (Figure 2-13D).

Over 1200 colonies were screened via colony lifts but none were found to have constructs containing either of the HindIII or SmaI PAR insertion sites. PCR for PAR was the only method I used to test for the presence of the PAR insertion sites in the plasmids. Restriction analysis was not performed on the plasmid preparations because I believed that the PAR PCR, which was used to generate the template for the PAR probe, was sufficient to identify plasmids carrying the PAR marker. It is possible however that there might have been something wrong with the plasmids that could have inhibited the PCRs. This could explain the conflicting results between the colony lifts and the PAR PCRs. Unfortunately this was not thought of at the time so the plasmids were not tested to see if this was the reason why the PAR PCRs were negative.

As I struggled to identify the flanking DNA of the PAR insertion sites I realized that a more targeted approach would give me a better chance of succeeding. To specifically target the PAR insertion sites in the 6.5kb SmaI and 7.5kb HindIII bands I needed to further characterize these insertion sites within the genome of the *adf1-3* rescue strain, so I attempted to map the insertion site through linkage analysis. As with the linkage analysis done on ADF1, my goal was to look at the recombination frequency between the PAR insertion site, through the presence of the PAR marker, and molecular markers spread across the genome. If I could narrow the location of the marker to an arm of a

chromosome, for example, then I might be able to use a more targeted approach to identify the DNA flanking the PAR insertion. I thus crossed the N1 strain to the polymorphic mapping strain S1D2 and recovered zygotes for tetrad analysis. Though the mating had generated hundreds of zygotes I soon found that none of them were able to germinate.

Normally following fusion of gametes the mated cells are plated and placed in the dark for 3 to 5 days, allowing for the zygotes to develop. The zygotes are then recovered and individual zygotes are spread on a solid media plate and exposed to light for 16 hours for germination to occur. I tried several conditions to induce germination of the zygotes I recovered from the N1 x S1D2 cross, but none were able to stimulate the zygotes into germinating. The S1D2 mating was also performed with different backcrossed progeny strains (from the *adf1-3* rescue x *adf1-1* cross) and the original *adf1-3* rescue strain but the zygotes would still not germinate.

It is unclear why the zygotes from the S1D2 mating could not germinate since I had no trouble recovering progeny from crossing the rescue strain with 137c (a WT strain) and *adf1-1*, as well as obtaining progeny from crossing N1 with 137c. It is possible that the answer lies with the polymorphic S1D2 strain. Due to its polymorphisms, and thus its use in mapping, S1D2 cannot be backcrossed (and has not been backcrossed since its identification). The strain therefore is rather sickly and can be difficult to work with. In all events I was unable to perform linkage analysis to map the PAR insertion site in the rescue strain.

2.4 Conclusion

Mutant *adf1* cells exhibit inactivation of the calcium-signalling pathway activated by intracellular acidification. Linkage analysis of the *adf1* mutant alleles map the ADF1 gene locus to a region on chromosome nine with 45 gene predictions. The initial goal of my Master's research was to rescue the *adf1* mutation with DNA from the ADF1 gene locus. When I recovered a potential rescue/suppressor in the *adf1-3* allele the goal changed to identifying the flanking DNA of the selectable marker used in the generation of the rescue. Despite not having been able to identify ADF1 or the DNA flanking the selectable marker in the *adf1-3* rescue strain, my work with ADF1 allows us to make two important observations: (1) it is likely that ADF1 lies in the 50kb sequence gap and (2) the putative *adf1-3* rescue is likely a suppressor.

As I laboured with ADF1 and the rescue/suppressor strain, a new deflagellation genetic screen was being carried out in the Quarmby lab. This screen uncovered a mutant with the *adf* phenotype, identifying a new gene, unlinked to the ADF1 locus. The following chapter describes the characterization and linkage analysis, which I have performed on this new gene.

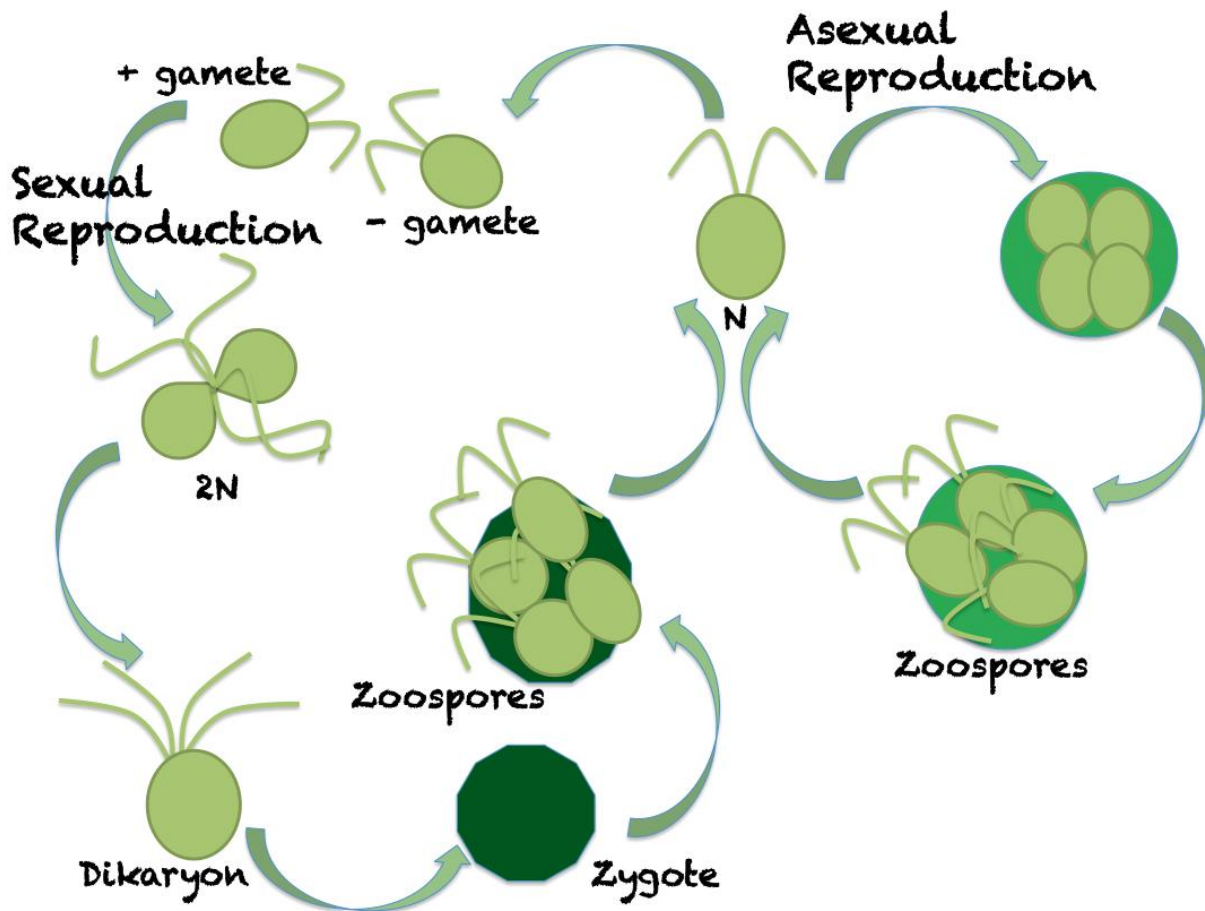


Figure 2-1: The *Chlamydomonas* life cycle.

Chlamydomonas undergoes both sexual and asexual reproduction. The haploid cells primarily reproduce asexually (mitosis), but under stressful conditions they undergo sexual reproduction. Maintaining cells on low nitrogen induces gametogenesis; gametes from strains of the two different mating types are then mixed allowing for fusion of mating type plus and minus gametes resulting in the formation of a temporary dikaryon. Once the zygote has formed it is enveloped by a protective wall. Zygote germination results in haploid vegetative cells, at this stage tetrad progeny can be recovered for genetic analysis.

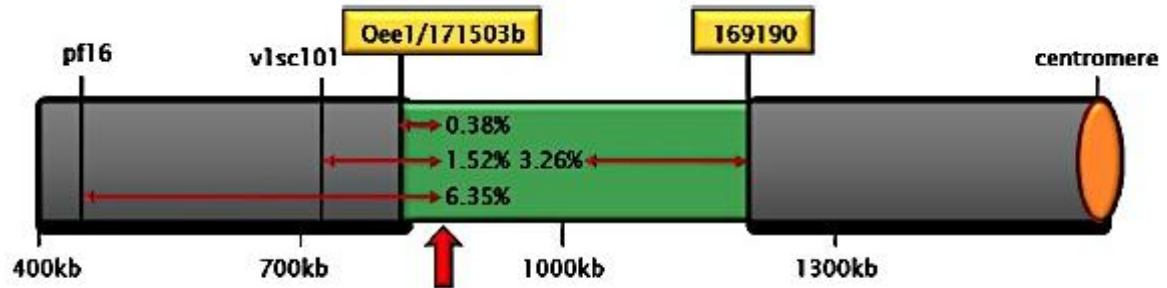


Figure 2-2: Linkage analysis of the ADF1 region.

The schematic depicts the boundaries of the ADF1 region (green) obtained by Jamie Kirschner through PCR-based recombination frequency mapping. Seventy-five progeny from tetrads were used to generate this map. Depicted are distances between ADF1 and several markers in map units. The red arrow indicates the center of mapping. Jamie Kirschner, 2009.

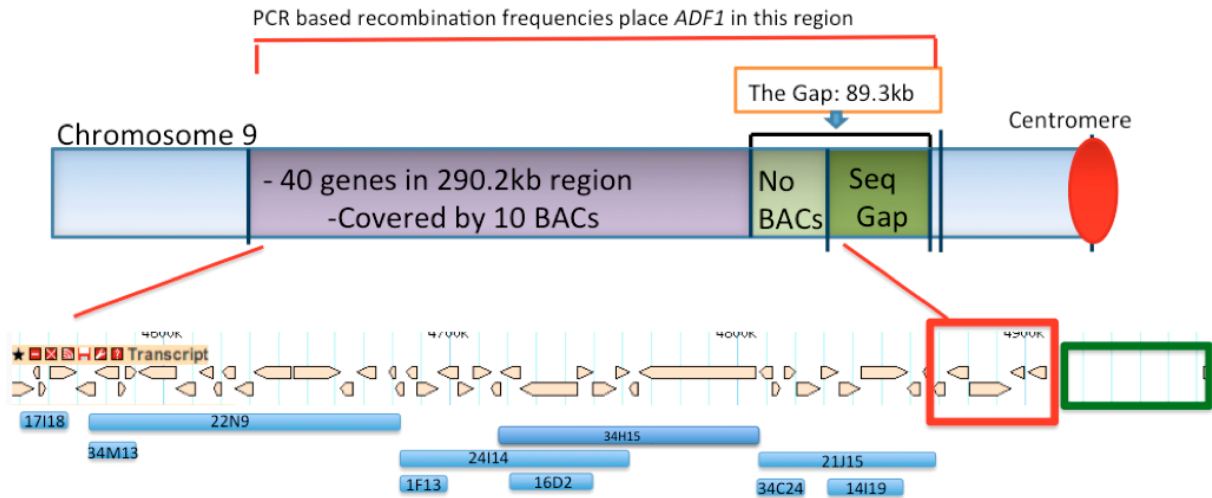


Figure 2-3: The *ADF1* gene locus.

In the current version of the *Chlamydomonas* genome browser the *ADF1* region lies in chromosome 9: 4576290-4957883. This region can be broken into three parts: (1) 290kb region consisting of 40 predicted genes covered by 10 BACs; (2) ~39kb region containing 5 predicted genes not covered by BACs; and (3) ~50kb region that contains no sequence in the annotated genome. The Augustus 10 gene predictions are shown in beige, BACs are in blue. The BAC(s) that covered the ~39kb region are not present in the BAC library from the *Chlamydomonas* Resource center.

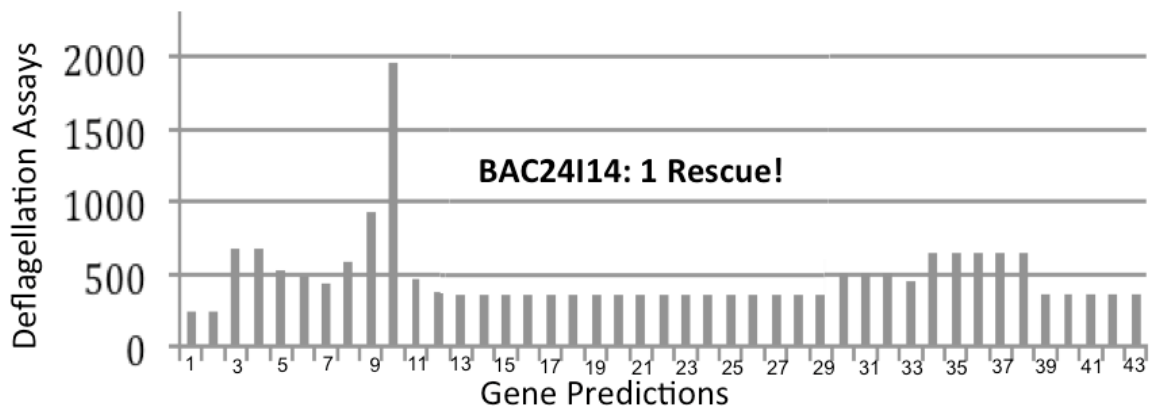


Figure 2-4: ADF1 phenotypic rescue assays

For gene predictions 1-38: assays were performed by co-transforming *adf1* mutant cells with digested BAC DNA and a linear selectable marker. These gene predictions are from the 290kb region. Gene predictions 39-43 were sub-cloned by Ziwei Ding and Adam Staniscia into a vector (pSI103) containing a selectable marker. The constructs were linearized prior to transformation. The selectable marker used was a paromomycin (PAR) resistant gene. The vector pSI103 was made by inserting the PAR gene into pBlueScript SK-.

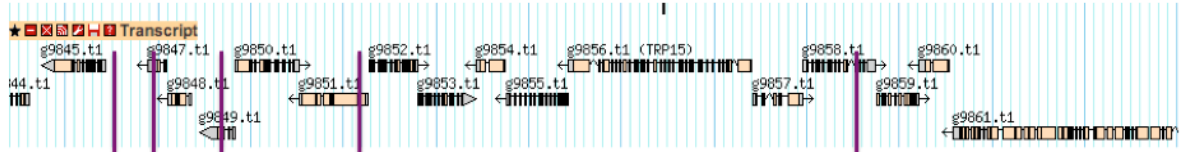


Figure 2-5: BAC24I14 Gene Predictions

BAC24I14 contains 15 full Augustus 10 gene predictions and partial coverage of a predicted ~40kb ATM/ATR-related phosphatidylinositol 3-kinase (only 23kb is present in BAC24I14). Of interest to us was gene prediction 22 (g9856.t1), which is predicted to encode a transient cation channel protein. The rescue with BAC24I14 of *adf1-3* was obtained by digesting BAC24I14 with EcoR1. Restriction sites are indicated in purple.

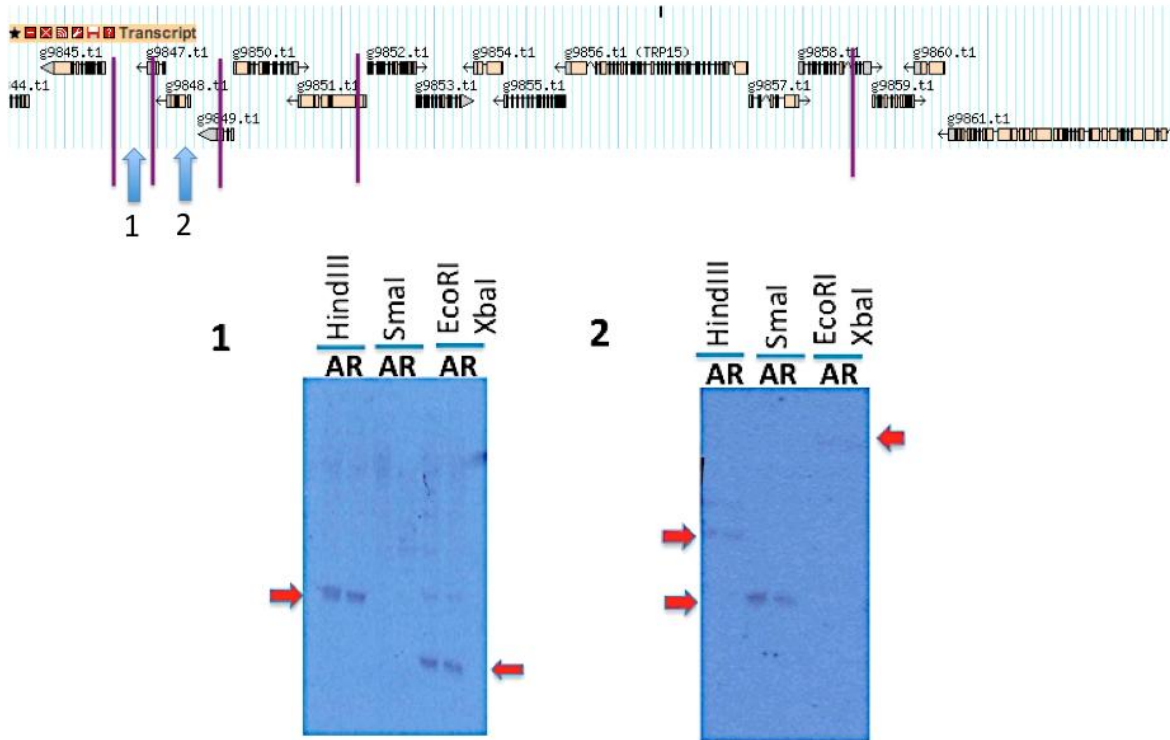


Figure 2-6: Southern analysis reveals single gene copy of two BAC24114 fragments in the genome of the *adf1-3* rescue strain.

Two radioactively labeled probes were made for gene predictions: g.9847 and g.9848 (note: g.9847 in the previous annotated genome was present in full in the region between the two EcoR1 cut sites). The original rescue strain was first backcrossed to *adf1-1* in the attempts to remove extra unlinked insertions of BAC or marker DNA; a wild-type deflagellation progeny was used for the southern (N1). The genomic DNA of N1 (R) and the parental *adf1-1* control (A) were then digested with several restriction enzymes and transferred to a nylon membrane for probe hybridization. Probes for both gene predictions were seen to hybridize in the same location in the genome for R and A strains indicating the presence of a single gene copy. Blue arrows: location of probes; purple lines: EcoRI cut sites.

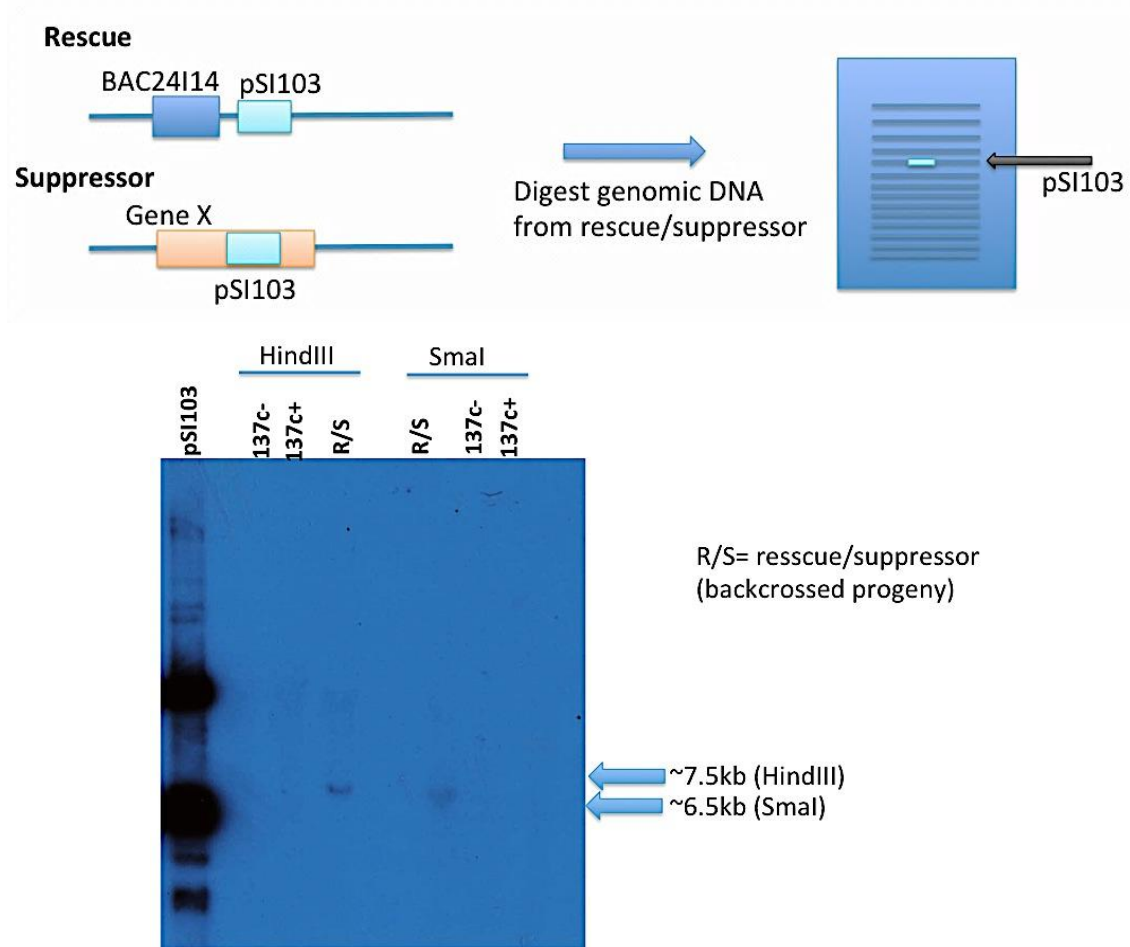


Figure 2-7: The PAR insertion site in the *adf1-3* rescue strain.

To find the site where the PAR marker inserted into the genome of the rescue/suppressor strain restriction analysis was performed. The genomic DNA was digested with HindIII and SmaI (separately) and probed with a radioactively labelled probe specific for PAR. (TOP) Schematic illustrating what the PAR insertion would look like if it were a suppressor or rescue. (BOTTOM) PAR southern blot reveals a ~7.5kb HindIII and ~6.5kb SmaI PAR insertions in the rescue/suppressor. pSI103: vector containing PAR marker; 137c +/-: wild-type strain that is PAR negative; R/S: rescue/suppressor strain. Note: a progeny from the *adf1-1/ adf1-3* rescue backcross was used- this strain was WT for deflagellation and PAR positive (N1).

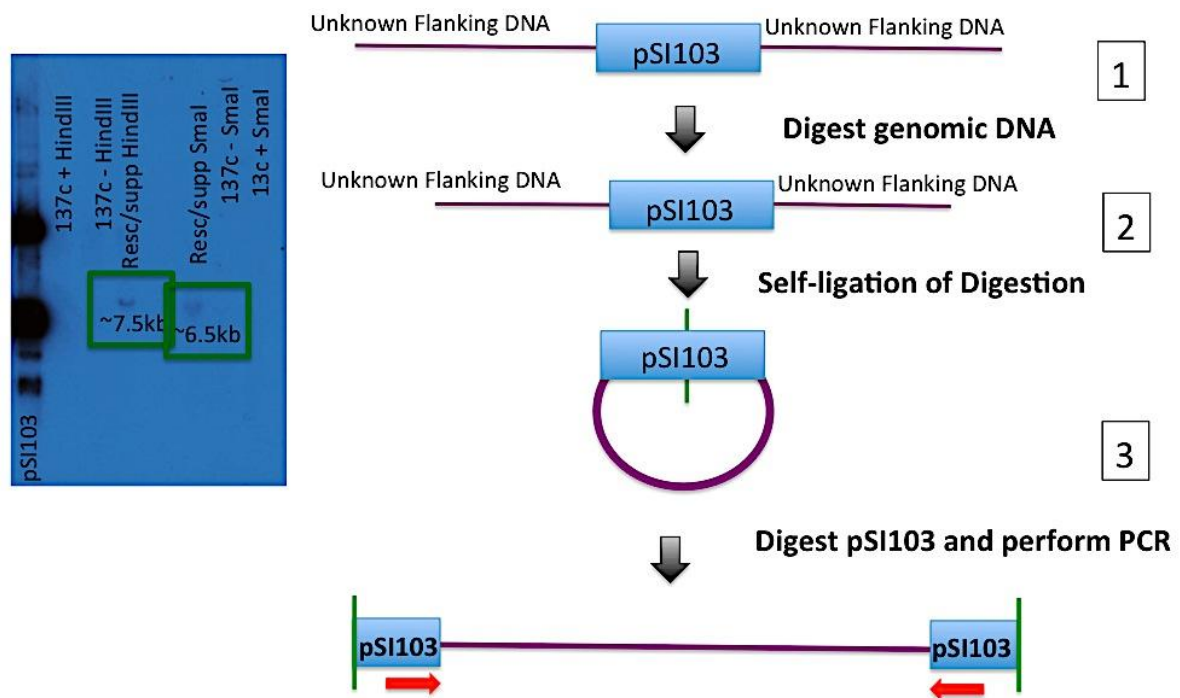


Figure 2-8: The Self-ligation PCR Method.

Schematic of the self-ligation PCR method. (LEFT) PAR southern blot showing the insertion sites. (RIGHT) Procedure for self-ligation PCR method: (1) genomic DNA is digested with HindIII and SmaI (separately) to produce the insertion sites. (2) Ligation is performed on the extracted bands, the ligation product is then digested with an enzyme known to cut inside the pSI103 vector. (3) PCR is performed with primers specific for the pSI103 vector. The PCR products can then be sequenced directly or ligated into a vector and then sequenced.

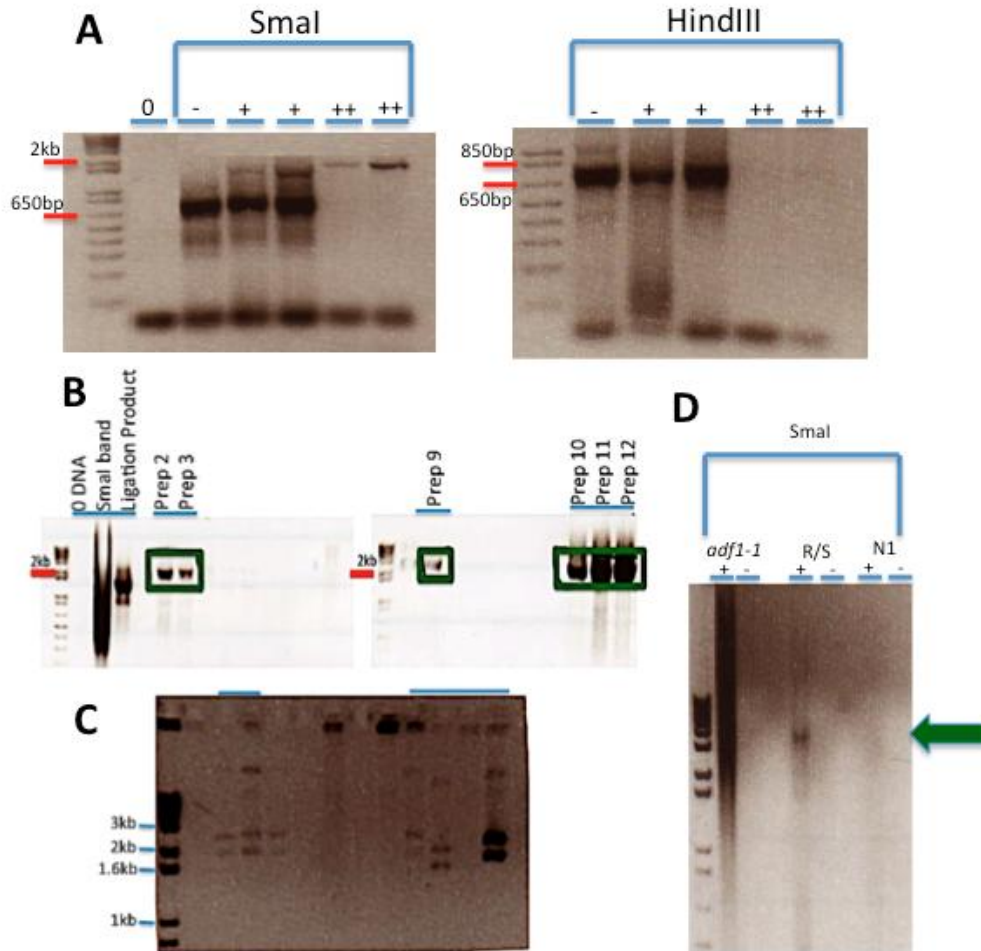


Figure 2-9: Self-ligation PCR identified a piece of BAC24114 beside a PAR insertion in the original *adf1-3* rescue no longer present in a backcrossed progeny strain.

Self-ligation PCR was performed on the original *adf1-3* rescue strain (R/S). A ~3kb band was amplified from the 6.5kb *Smal* PAR insertion site. This band was found to contain a fragment of BAC24114. When the method was performed on a backcrossed progeny strain (N1: WT for deflagellation & PAR+) the 3kb was not present, indicating that this fragment is not involved in the rescuing phenotype of *adf1-3*. (A) Self-ligation PCR was performed on the original *adf1-3* rescue strain. The 7.5kb *HindIII* and 6.5kb *Smal* bands were either self-ligated (+) or not (-), then digested with *BamHI* prior to PCR. For the *Smal* PAR insertion site a ~3kb and ~700bp (non-specific) bands were amplified. The PCR cycling conditions were modified to amplify only the ~3kb band (++) . (B-C) The ~3kb band was ligated into pGEMT, PCR and restriction analysis (with *BamHI*) were performed to detect positive constructs. For the restriction analysis the construct was expected to produce a 3kb band (vector backbone) and a 3kb band (PCR insert). (D) Self-ligation PCR was then performed on a backcrossed progeny (N1). Note: N1 is the same strain used in the PAR southern done to identify the PAR insertion sites; the 1kb plus ladder from Invitrogen (Burlington, Canada) was used.

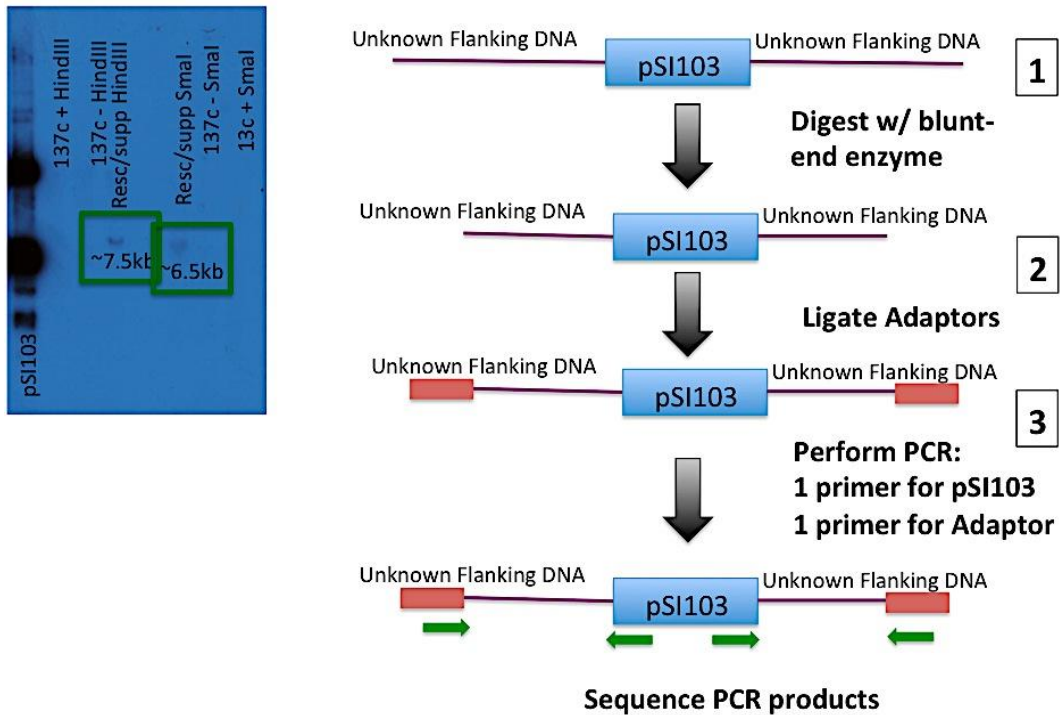


Figure 2-10: The TAIL-Adaptor PCR Method.

Schematic of the TAIL-Adaptor PCR method (Adapted from Iomini et al., 2009). (LEFT) PAR southern blot showing the insertion sites. (RIGHT) Procedure for TAIL-Adaptor PCR: (1) the insertion sites were further digested with a restriction enzyme to create blunt ends. (2) DNA adaptors were ligated to the blunt ends of the insertion sites. (3) PCR was performed with primers that were specific for the adaptor and for the PAR marker in pSI103. The PCR products were then either ligated into a vector or sent for sequencing directly.

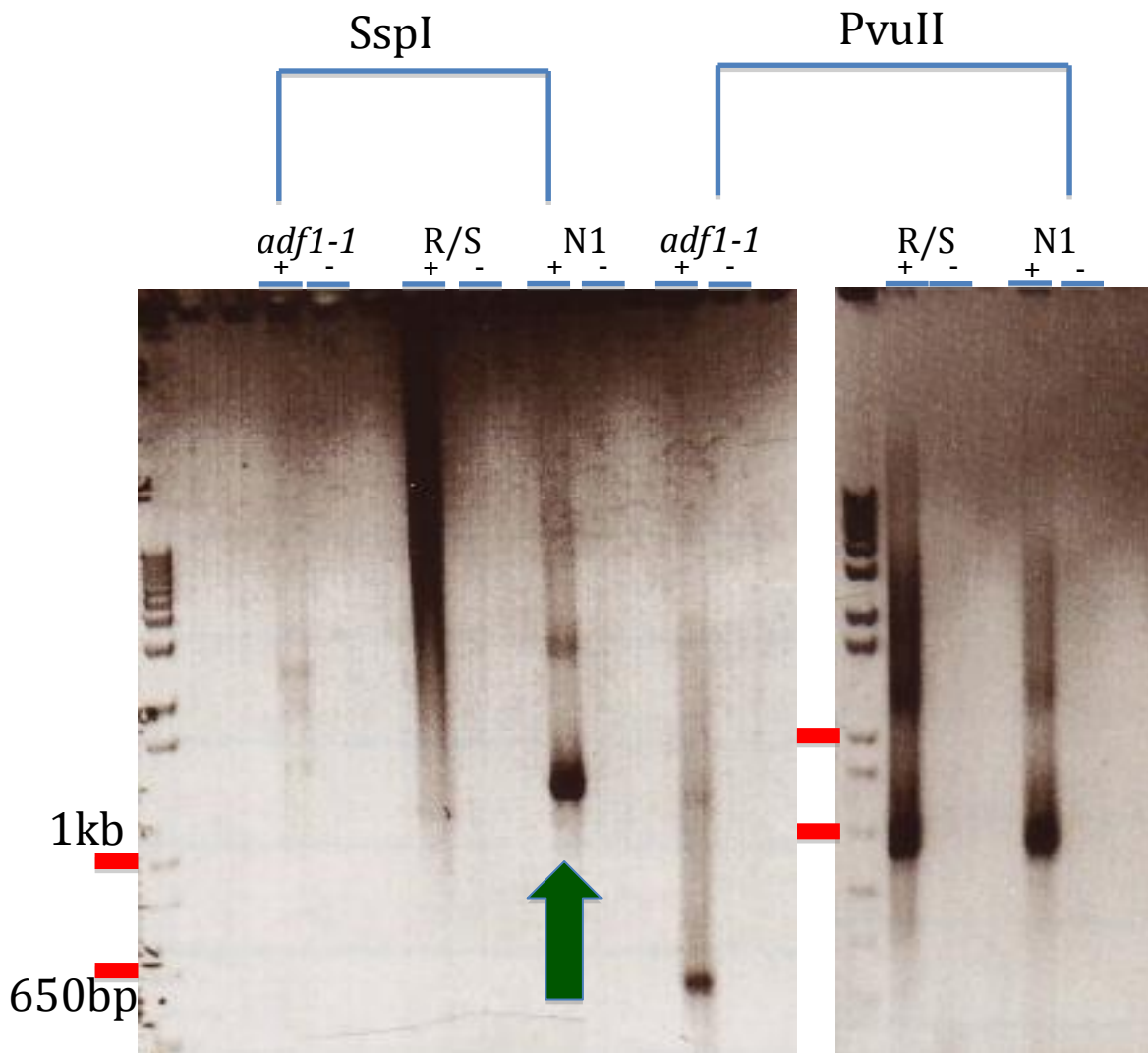


Figure 2-11: TAIL-Adaptor PCR amplified a ~1.3kb band from the 6.5kb SmaI PAR insertion site

Using TAIL-Adaptor PCR (Iomini et al., 2009) a ~1.3kb band was amplified from the 6.5kb SmaI PAR insertion site (green arrow). Attempts were done to ligate the band into pGEMT prior to sequencing but were unsuccessful. The PCR product was sent in for sequencing but no sequence was generated. TAIL-Adaptor PCR was performed on a *adf1-1* control, the original *adf1-3* rescue strain (R/S) and a progeny strain (N1) from the *adf1-1/adf1-3* rescue WT for deflagellation and PAR positive. Blunt ends were generated by digesting the X insertion site with SspI or PvuII. PCR was performed on strains with (+) and without (-) adaptors. Red bars indicate 1kb and 650bp. Note: N1 is the same strain used in the PAR southern done to identify the PAR insertion sites.

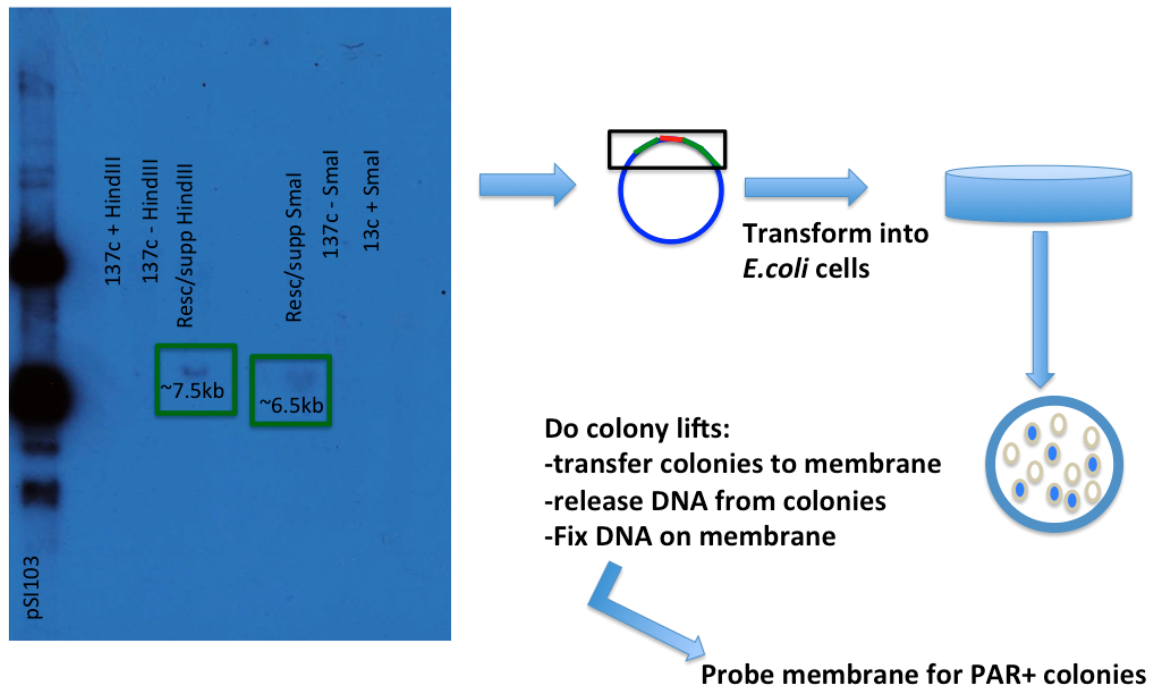


Figure 2-12: The Colony Lift Method

Schematic of the colony lift method. The bands containing the PAR insertion sites were sub-cloned into pBlueScript (SK-) and then transformed into chemically competent Mach1 *E. coli* cells. The cells were then transferred onto a membrane and the DNA from the colonies was released and fixed. The membranes were then probed using the radioactive PAR probe used to identify the PAR insertion sites.

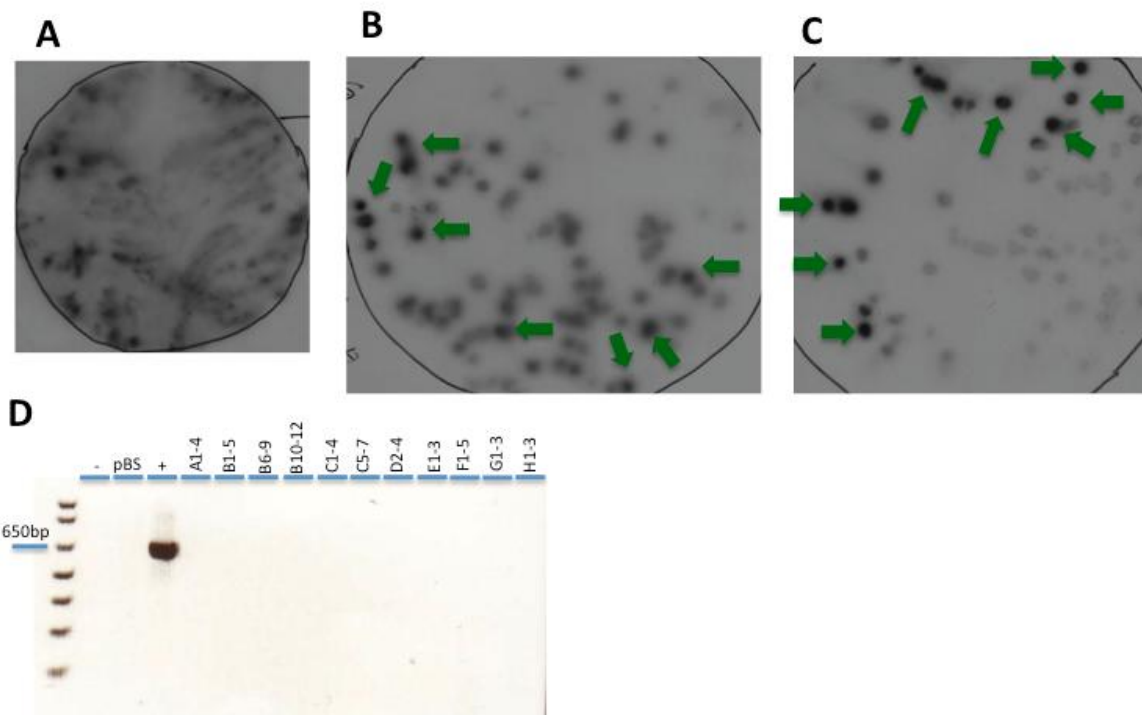


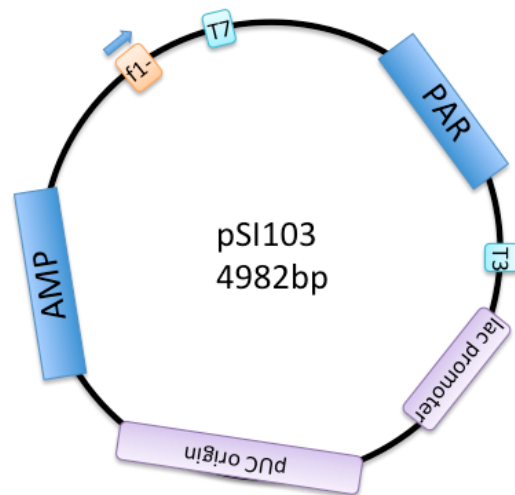
Figure 2-13: Colony lifts were used to try and identify bacteria containing constructs with the PAR insertion sites.

The PAR insertion sites (7.5kb HindIII and 6.5kb SmaI bands) were ligated into pBlueScript and transformed into chemically competent Top10 *E.coli* cells. The colonies were then transferred to a membrane and probed with the PAR specific probe. (A) Vector control was performed by transforming cells with pBlueScript and a dilute amount of pSI103. Though the transfer was smeary minimal signal was detected with the PAR probe consistent with dilute amount of pSI103. (B-C) Colony lifts of cells transformed with constructs containing the 6.5kb SmaI PAR insertion site (B) and the 7.5kb HindIII PAR site (C). Colonies with strong signals (green arrows) were further analyzed: plasmid extractions were performed and PCR was then done on the plasmids for PAR (D). As seen, only the pSI103 (+) was positive for PAR, negative controls were performed with no DNA (-) and with pBlueScript (pBS), subclones A-C are were extracted from colonies transformed with SmaI bands, D-H with HindIII.

Supplemental Data

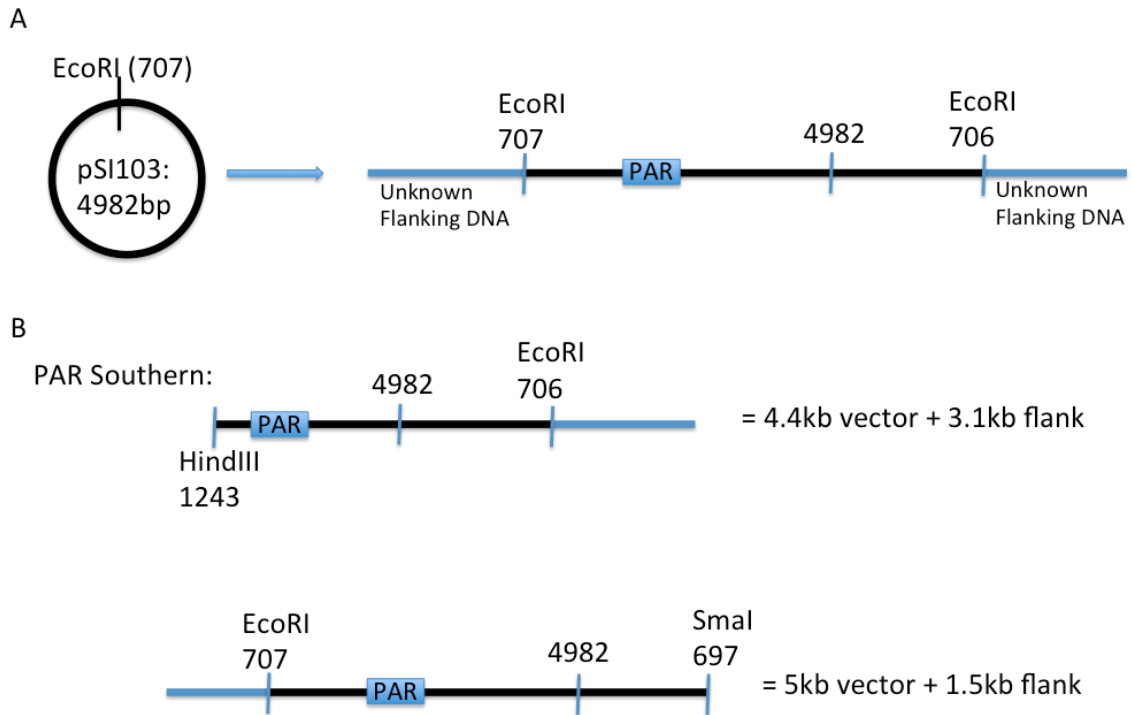


F1- origin of ss-DNA replication: 21-327
T7 promoter initiation site: 643
PAR resistance gene: 1665-2468
T3 promoter initiation site: 2799
Lac promoter: 2842-2963
pUC origin: 3183-3850
AMP resistance gene: 3964-4824



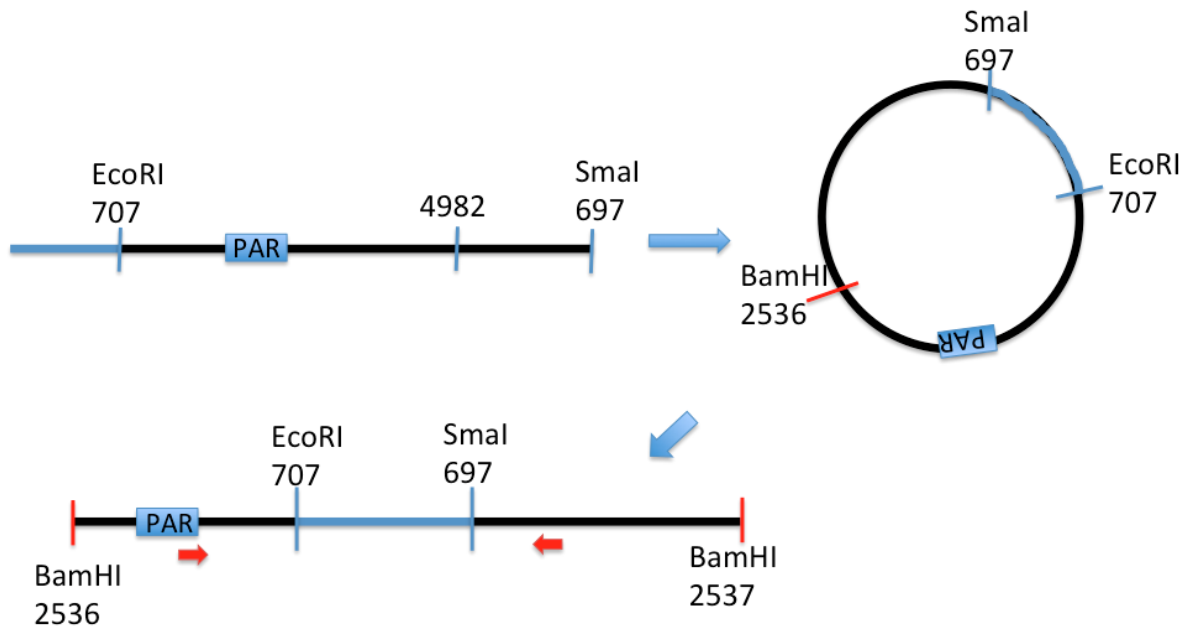
Supplemental 2-1: pSI103

Schematic of the vector components of pSI103, which was used in the phenotypic rescue assays to identify ADF1. The vector was constructed by inserting the Paromomycin resistance gene (PAR) into the multiple cloning site (MCS) of pBlueScript SK-.



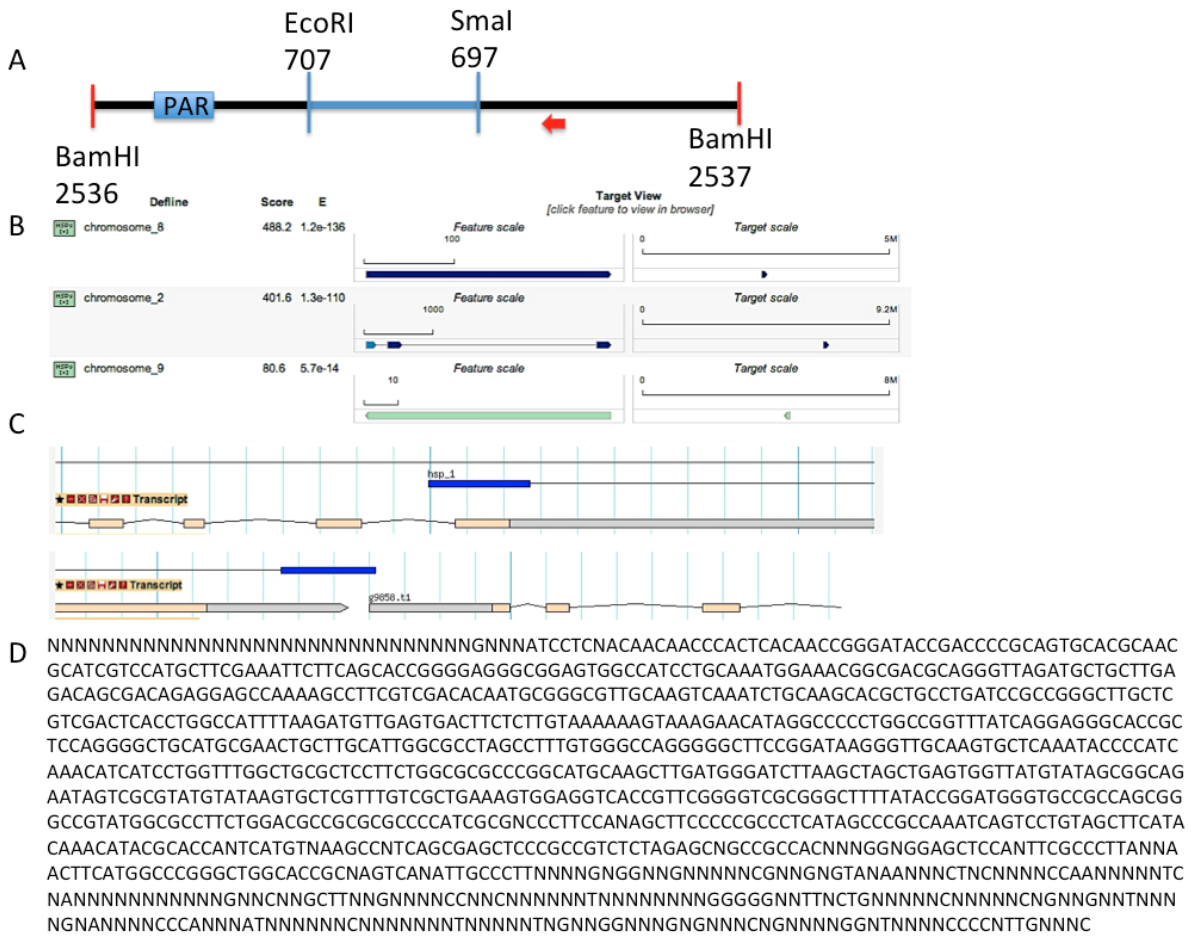
Supplemental 2-2: The PAR insertion sites generated in the PAR southern blot

(A-B) Schematic of the PAR insertion sites in the *adf1-3* rescue strain, identified in the southern blot. PAR: paromomycin resistance gene.



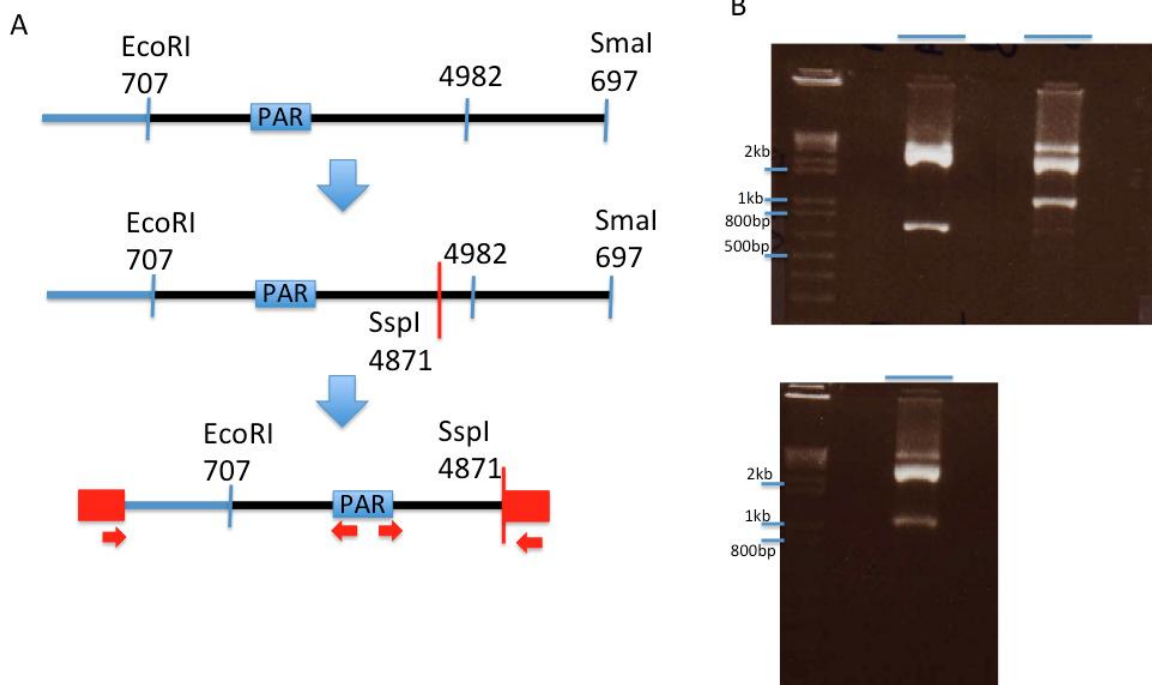
Supplemental 2-3: The Self-ligation PCR product from the 6.5kb SmaI PAR insertion site

Schematic of the construct generated through the self-ligation PCR method. The primers used to amplify the flanking DNA were specific for the PAR marker and the ampicillin resistance gene in the vector backbone (primers indicated by red arrows).



Supplemental 2-5: The self-ligation PCR method amplified a fragment of BAC24I14 in the original *adf1-3* rescue strain using an AMP specific primer.

(A) Schematic of the self-ligation PCR product from the 6.5kb *SmaI* PAR insertion site, which was sent to Eurofins MWG Operon (Louisville, USA) for automated sequencing. Sequencing primer: primer for the ampicillin resistance gene (AMP) was used to amplify the product (red arrow). (B-C) BLAST results from blasting the sequencing results from (A) to the *Chlamydomonas* genome in Phytozome. The product blasted to chromosome 8 (heat shock protein, C top) and to chromosome 9 (g9857, C bottom). (D) The sequencing data generated from the self-ligation PCR product (with the AMP primer).



Supplemental 2-6: The TAIL-Adaptor PCR method generated a 1.3kb product, which appeared to be sub-cloned into pGEMT.

(A) Schematic of the product created through the TAIL-Adaptor PCR method (Iomini et al., 2009). The PCR product was 1.3kb indicating that the PCR amplified the flanking DNA plus vector (to the left of PAR). (B) Restriction analysis of three constructs sent for sequencing. The constructs were tested to see if they contained the 1.3kb TAIL-Adaptor PCR band by restriction digest with SspI where the band would either be released resulting in a 3kb and 1.3kb band, or where the digest would yield a 2.8kb and 182bp band (empty vector). Though the resulting bands were found to be smaller than 1.3kb the constructs were still sent out for sequencing, but only vector sequence was recovered.

References

Finst RJ, Kim PJ, Quarmby LM: Genetics of the Deflagellation Pathway in Chlamydomonas. *Genetics* 149: 927-936, 1998

Iomini C, Till JE, Dutcher SK: Genetic and Phenotypic analysis of flagellar mutants in Chlamydomonas reinhardtii. *Methods in Cell Biology* 93: 121-143, 2009

Kirschner, Jaime: Mapping the Deflagellation-defective ADF1 gene in Chlamydomonas reinhardtii. Msc Thesis. 2009

3. ADF2: The acid deflagellation gene 2

3.1 A new deflagellation genetic screen and a new ADF gene

The mechanism of acid-induced deflagellation can be broken down into three steps: (1) the activation of extracellular calcium influx triggered by intracellular acidification, (2) a calcium signalling pathway resulting in the release of intracellular calcium stores and (3) the activation of the microtubule severing machinery leading to the shedding of the cilium. From this we can infer that a calcium sensing/binding protein and an axonemal microtubule severing protein must be involved in deflagellation. Despite being saturated, no such genes were recovered in the 1998 deflagellation genetic screen (Finst et al., 1998). If these genes, however, are involved in both deflagellation and in the severing of the axoneme during pre-mitotic reabsorption, then it is possible that these genes are essential for cell survival. If this is true then it is likely that these mutants were not recovered in the Finst screen because null mutations in these genes, like those generated in FA1 and FA2, would have been lethal.

To overcome this obstacle the Quarmby lab conducted a second deflagellation genetic screen in the summer of 2012, looking for conditional deflagellation mutants. Four research assistants carried out the screen: Fabian Garces, Fabian Meili, Paul Buckoll and Mihajlo Todorovic. Using UV mutagenesis the screen aimed at generating deflagellation mutants that at a permissive temperature would be viable but upon shifting to the restrictive temperature the mutant phenotype would be observed. To more efficiently

recover these rare conditional mutants the screen employed an phototaxis enrichment step where the cells, following UV mutagenesis, were exposed to acid deflagellation buffer to induce deflagellation then allowed to phototax towards a light source. In this way the deflagellation mutants, who retain their flagella and can thus swim towards the light source, were separated from the non-deflagellation mutant cells, which did deflagellate.

This new screen recovered 21 deflagellation mutants: two temperature sensitive mutants and 19 non-temperature sensitive mutants (Table 3-1). Of the 19 non-conditional mutants six displayed the FA phenotype: two were found to be alleles of FA1 while the other four are alleles of FA2. The thirteen other mutants exhibited the ADF phenotype, six of which are confirmed alleles of ADF1, while the remaining seven are still being characterized. One of the conditional mutants exhibited the ADF phenotype while the second mutant displayed a mix phenotype- temperature sensitive FA mutant and non-conditional ADF1.

To see if the conditional *adf* mutant, temporarily named N23, was a new allele of ADF1 I performed complementation analysis on N23/*adf1-1* dikaryons. In the sexual reproductive cycle of *Chlamydomonas*, gamete fusion yields the formation of a temporary dikaryon, which retains both set of flagella and both nuclei. These dikaryons are great genetics tools to test if the components of one of the cell's flagella can rescue the other pair of flagella. Complementation analysis had previously been performed on *adf1*/ADF1 (WT) dikaryons and stable diploids (Finst et al., 1998). All four flagella were shed in the dikaryons, thus, the WT flagellar components were able to rescue the *adf1* mutant flagella, and none of the diploids were deflagellation defective indicating that the *adf1* phenotype is recessive.

To test if the mutation in N23 could be complemented by WT components, N23 was mated with a wild-type strain (137c) and the dikaryons were then tested for their ability to shed their flagella. Deflagellation of both pair of flagella was observed for the dikaryons that formed, indicating that a WT component was sufficient to restore the ability to deflagellate to N23 flagella. Given the ability of WT flagella to rescue *adf1* and the recessive nature of the mutation, I hypothesized that if the N23 mutant was a new allele of ADF1 then the N23/*adf1-1* dikaryons would not be able to shed their flagella. If, however, N23 was a novel ADF gene then its WT ADF1 copy would be able to rescue the *adf1* flagella and vice versa, thus, the dikaryon would be able to shed all four flagella (Figure 3-1A). Shortly after inducing deflagellation I observed that the N23/*adf1-1* dikaryons lost all four of their flagella, indicating that complementation had occurred (Figure 3-1B). From these results we can conclude that N23 is likely a new deflagellation gene involved in the calcium-signalling pathway, which we have named ADF2.

3.2 Linkage Analysis of ADF2

To further characterize the conditional *adf* mutant I performed linkage analysis. As with the mapping of ADF1, *adf2-1* was crossed to the polymorphic mapping strain S1D2. The progeny from nine zygotes were recovered and screened for deflagellation; their genomic DNA was then extracted in preparation for PCR. A mapping kit, from the Chlamydomonas Resource center, was used for primary linkage analysis (Kathir et al., 2003). Using this mapping method, I assessed linkage between the ADF2 gene and molecular markers along the 17 chromosomes.

For the majority of the markers I observed segregation frequencies between 45-65% (Figure 3-2) indicating no linkage between the markers and the ADF2 gene. Based on the rate of recombination between ADF2 (*adf2* phenotype) and the molecular markers, I was able to establish linkage between ADF2 and CNA34 on linkage group (LG) III, where recombination frequency was 0%. It should be noted that there were three markers on other linkage groups (ALD, EST894011B10 and IDA2) that had low recombination frequencies (below 30%). I am unclear why such low recombination frequencies were obtained for these markers; however, given that CNA34 exhibited 0% recombination I focused on LG III. ADF2 is not linked to LG IX, the location of ADF1, confirming that this conditional mutant has uncovered a new deflagellation gene.

To narrow down the location of the ADF2 gene locus I created several molecular markers that spanned on either side of CNA34 (Figure 3-3). These markers were made by amplifying ~1kb introns from predicted genes in the region and digesting with HaeIII, HhaI or MspI, individually. Using the progeny from the *adf2-1/S1D2* zygotes I was able to map the locus to a 1.85Mb region from chromosome 3: 6266545-8124216, between markers 2A and 9A (Figure 3-3A, Table 3-2). To further refine the location of ADF2 more recombinant progeny needed to be analyzed so I performed bulk zygote dissections on zygotes from the *adf2/S1D2* cross. These dissections were done by first transferring individual zygotes (~200) unto a fresh TAP plate prior to placing them in a 15mL falcon tube containing liquid TAP. This transfer was performed to eliminate vegetative cells from contaminating the progeny following zygote germination. The zygotes were then placed in front of bright lights for 72hours to induce germination and plated (~700uL) on solid media.

From the bulk zygote dissections, 250 colonies were picked and analyzed for the *adf2* deflagellation mutant phenotype. Cells were inoculated into 150uL liquid TAP in 96-

well plates and incubated for 24 hours at 21°C followed by 8 hours at 33°C. I was unable to assay the majority of the strains because at the restrictive temperature they were unable to hatch following division, and thus their flagella were not exposed to the acidic environment. From the 250 colonies recovered I was only able to assign phenotypes to 63 strains. Of the 63 colonies 28 exhibited the *adf2* phenotype; the 63 strains were then grown and their genomic DNA was isolated for PCR. The 28 *adf2* progeny all exhibited 0% recombination between the *adf2* phenotype and the molecular markers. From the 35 S1D2 progeny a double recombination event (between markers 7A and 8B, and 8.4B and 8.5B) was found on strain #22, indicating that ADF2 lies either to the left of 7A or to the right of 8.5B. Given this recombination event the ADF2 locus is located in either a: (1) 437.8kb region on chromosome 3: 6266545-6695119, or a (2) 1.4Mb region on chromosome 3: 6704360-8124216.

3.3 Conclusion

Thirty years ago the first flagellar autotomy mutant, *fa1-1*, was recovered from a UV mutagenesis screen for deflagellation (Lewin and Burrascano, 1983). Since then only two other genes have been identified to play a role in the process of deflagellation: FA2 and ADF1. The mechanism leading to axonemal severing, however, indicates that more genes are present to carry out this chemical stress response. To discover the other genes in the deflagellation pathway a conditional deflagellation genetic screen is being performed in the Quarmby lab.

From this screen I characterized a temperature sensitive mutant (N23), which exhibited the *adf* deflagellation phenotype at the restrictive temperature, but was wildtype at normal growth temperatures. Through complementation analysis in temporary dikaryons and linkage analysis I determined that the mutation is a novel gene, hereby named ADF2, involved in the proton-activated (*adf*) calcium-signalling pathway that leads to the activation of the microtubule severing machinery. Though the Quarmby lab has hypothesized that additional genes involved in deflagellation would be essential for cell survival ADF2 was not found to have any growth phenotypes at the restrictive temperature (data not shown), indicating that ADF2 is a non-essential gene for *Chlamydomonas* cell survival. But if ADF2 is not essential then why was it not recovered in the original 1998 genetic screen? We don't yet know, but two possibilities are: (1) ADF2 was not found in the insertional mutagenesis screen due to ADF2 being a small gene thereby decreasing the probability of the insertional tag landing inside of the gene. Or, (2) ADF2 lies in a region of the genome that has a low frequency of insertion.

To identify the ADF2 gene I used PCR-based recombination frequency mapping (linkage analysis) was able to map the ADF2 gene locus to a 1.85Mb region on chromosome 3: 62665454-8124216. A fortuitous double crossover event revealed that ADF2 lies either in a 437.8kb region on chromosome 3: 6266545-6695119, or in a 1.4Mb region on chromosome 3: 6704360-8124216. To determine which of these two regions the ADF2 gene is in linkage analysis needs to be performed on more *adf2/S1D2* progeny. Once we ascertain where the ADF2 locus is the next step would be to use sequencing and bioinformatics to identify nucleotide polymorphisms between the ADF2 genome and the 137c wild type reference genome to discover potential mutations in candidate genes in the

ADF2 gene locus. These candidate genes will then be tested using phenotypic rescue assays to identify the ADF2 gene.

Phenotype	ADF		FA		Other
Mutants recovered	14		6		1
Gene	<i>ADF1</i>	<i>ADF2</i>	<i>FA1</i>	<i>FA2</i>	<i>C7</i>
Alleles	6	1	2	4	1

Table 3-1: The Deflagellation Mutants Recovered in the 2012 Conditional Genetic Screen

Complementation analysis in dikaryons was performed for the *adf* mutants to determine if they were alleles of *ADF1*. The *fa* mutants were crossed with *fa1* and *fa2* and tetrad analysis was performed to determine if they were new alleles of *FA1* or *FA2*. The mutant *C7* was found to have a mixed phenotype where at the permissive temperature it exhibits the *adf* phenotype whereas at the restrictive temperature behaves as a *fa*.

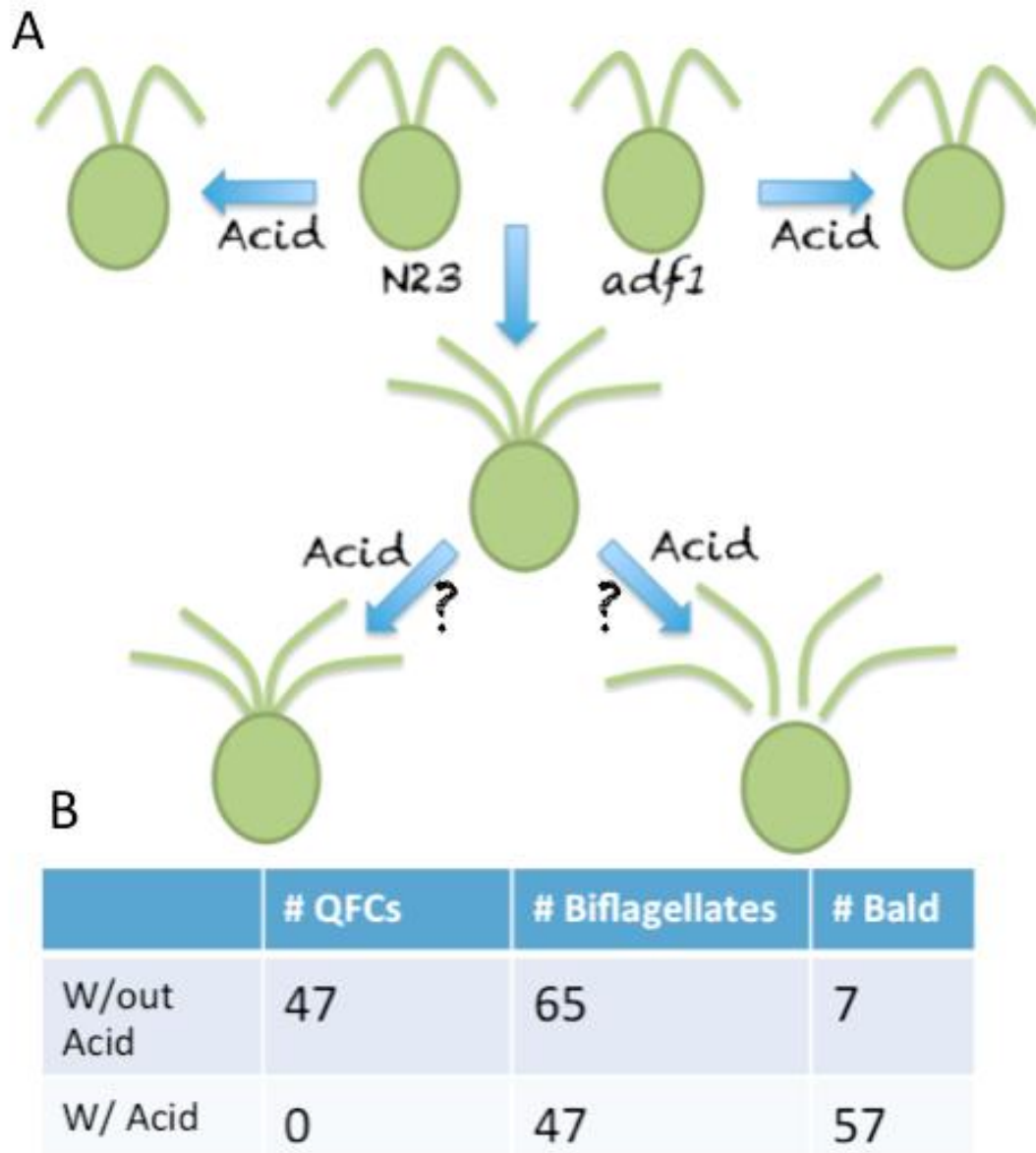


Figure 3-1: Complementation analysis in dikaryons reveals a new gene, ADF2, involved in the calcium-signalling step in deflagellation.

(A) Schematic illustrating the complementation experiment between ADF1 and the N23 temperature sensitive mutant recovered in the conditional genetic screen. (B) Table with the data from the complementation results between N23 and *adf1-1*. The number of QFCs (quadriflagellate cells) indicates the cells that successfully mated and formed dikaryons; biflagellate are cells that did not mate. When acid was added the QFCs were seen to deflagellate indicating complementation had occurred.

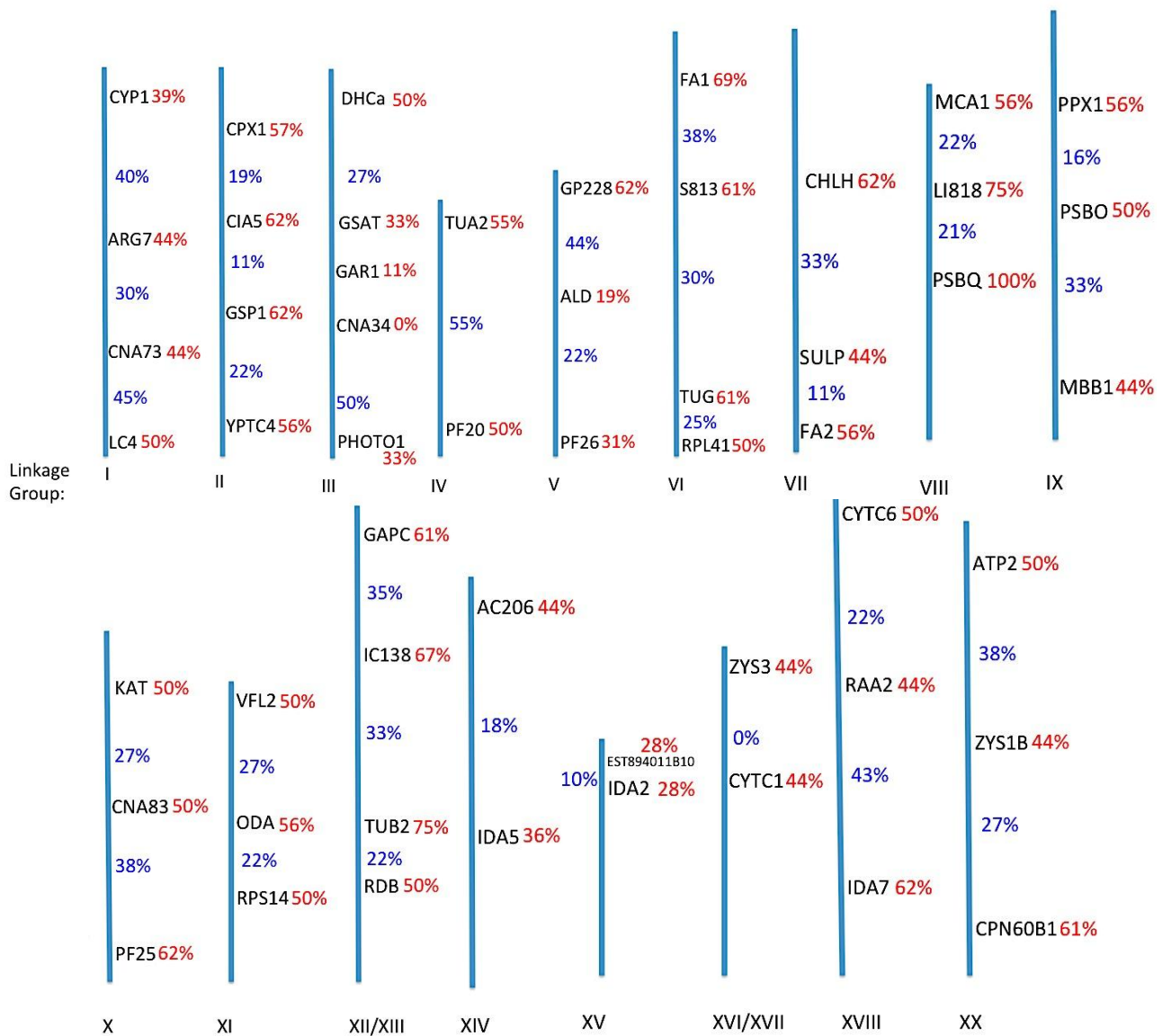


Figure 3-2: Linkage analysis places ADF2 on chromosome 3.

To map the ADF2 gene, *adf2-1* was crossed to the polymorphic mapping strain S1D2. Progeny from ten tetrads were then used for PCR-based recombination frequency mapping. Linkage was seen between ADF2 and the molecular marker CNA34 on linkage group (LG) III. Markers LI818 and PSBQ, on LG VIII, exhibited high levels of recombination between them and ADF2- this could be due to the markers being in a region of high recombination in the genome. Segregation frequencies between ADF2 and molecular markers are in red; recombination between markers is in blue. The *Chlamydomonas* mapping kit from the *Chlamydomonas* resource center was used (St. Paul, MIN, USA) (Kathir et al., 2003).

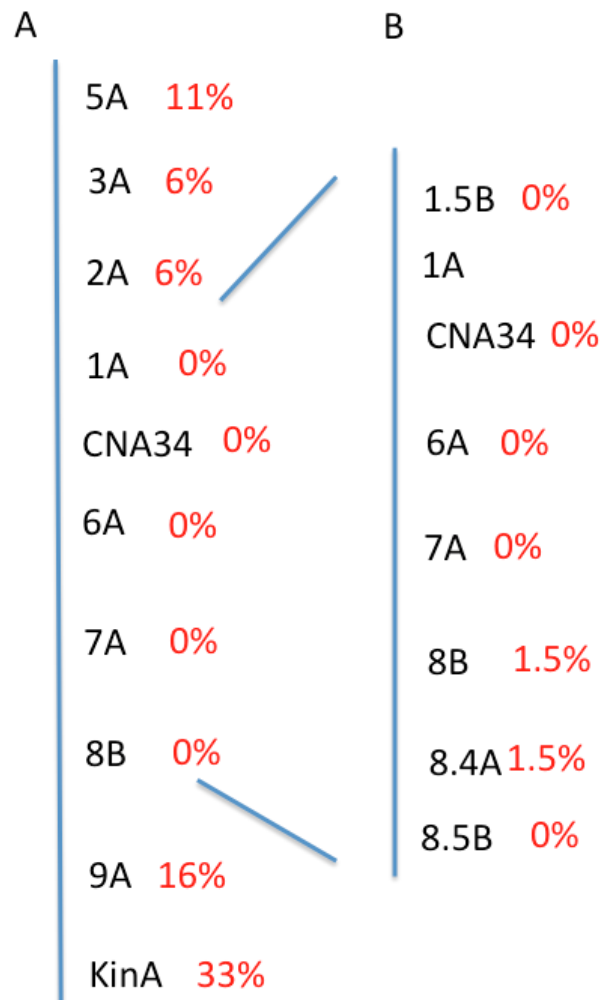


Figure 3-3: Linkage analysis places ADF2 between either: (1) markers 2A and 7A or (2) markers 8.4A and 9A.

Molecular markers were made for genes to the left and right of CNA34. (A) Linkage analysis was performed with the molecular markers on the progeny from the 9 zygotes (from the *adf2*/S1D2 cross). This initial mapping shows that ADF2 lies between 2A and 9A. (B) Linkage analysis was performed on 63 random progeny from a bulk zygote dissection of the *adf2*/S1D2 cross. A double recombination event in one of the S1D2 progeny (between markers 7A and 8B, and 8.4A and 8.5B) narrowed down the ADF2 gene locus indicating that ADF2 lies either between marker 2A and 7A, or between 8.4A and 9A.

Table 3-2: Linkage Analysis of the progeny from the nine *adf2-1/S1D2* zygotes.

Zygotes from an *adf2-1/S1D2* cross were dissected and the progeny recovered (note: I was unable to dissect zygotes at the tetrad stage, progeny recovered were from zygotes dissected at the 8 and 16 cell stage). Linkage analysis was performed on the progeny strains using molecular markers generated through PCR and restriction digest (1, 2, 3, 5, 6, 7.1, 7, 8, 8.5, 9 and KIN). The progeny strains exhibiting the four genotypes from each zygote are shown in the table. Molecular markers are indicated on the top row. Recombination frequencies between the ADF2 phenotype and the molecular marker for each strain are shown directly below the genotypes for each zygote, followed by intra-marker recombination. Total recombination frequencies (for both ADF2/marker and marker/marker) are seen in the last two rows of the table (respectively). Blank cells indicate missing genotypes. S1D2: indicates the presence of the polymorphic genotype (green); 137c: indicates the presence of the non-polymorphic genotype (blue); WT: indicates the wild type deflagellation state (orange); ADF2: indicates the presence of the non-deflagellation state (purple); Ghost: indicates the progeny strain missing for that zygote that would complete the tetrad.

Phenotype	Progeny	LG3	DHCa	GSAT	SAC1+2	GAR1	5	3	2	1	CNA34	6	7.1	7	8	8.5	9	KIN	PHOT1	
ADP2	A1	S1D2	S1D2	137c	137c	137c	137c	137c	137c	137c	137c	137c	137c	137c	137c	137c	137c	s1d2	s1d2	S1D2
WT	A3	137c	137c	137c	S1D2	S1D2	S1D2	S1D2	S1D2	S1D2	S1D2	S1D2	s1d2	S1D2	S1D2	s1d2	s1d2	s1d2	s1d2	S1D2
WT	A6	S1D2	S1D2	S1D2	S1D2	S1D2	S1D2	S1D2	S1D2	S1D2	S1D2	S1D2	s1d2	S1D2	S1D2	s1d2	s1d2	137c	137c	137c
ADP2	A9	137c	137c	137c	137c	137c	137c	137c	137c	137c	137c	137c	137c	137c	137c	137c	137c	137c	137c	137c
		0.5	0.5	0.5	0	0	0	0	0	0	0	0	0	0	0	0	0.5	0.5	0.5	0.5
		0	0	0	0.5	0	0	0	0	0	0	0	0	0	0	0	0.5	0	0	0
WT	GHOST	S1D2	S1D2	S1D2	S1D2	S1D2	S1D2	s1d2	S1D2	S1D2	S1D2	S1D2	s1d2	S1D2	S1D2	s1d2	s1d2	137c	137c	137c
ADP2	B2	S1D2	137c	137c	137c	137c	137c	137c	137c	137c	137c	137c	137c	137c	137c	137c	137c	s1d2	137c	S1D2
WT	B4	137c	S1D2	S1D2	S1D2	S1D2	S1D2	s1d2	S1D2	S1D2	S1D2	S1D2	s1d2	S1D2	S1D2	s1d2	s1d2	s1d2	s1d2	S1D2
ADP2	B5	137c	137c	137c	137c	137c	137c	137c	137c	137c	137c	137c	137c	137c	137c	137c	137c	137c	137c	137c
		0.5	0	0	0	0	0	0	0	0	0	0	0	0	0	0	0	0	0	0.5
		0.5	0	0	0	0	0	0	0	0	0	0	0	0	0	0	0.5	0	0	0
ADP2	C2	137c	137c	s1d2	137c	137c	137c	137c	137c	137c	137c	137c	137c	137c	137c	137c	137c	137c	137c	137c
WT	C4	137c	137c	137c	137c	137c	S1D2	S1D2	S1D2	S1D2	S1D2	S1D2	s1d2	S1D2	S1D2	s1d2	s1d2	s1d2	s1d2	S1D2
ADP2	C7	s1d2	s1d2	137c	137c	137c	137c	137c	137c	137c	137c	137c	137c	137c	137c	137c	137c	137c	137c	137c
WT	GHOST	s1d2	s1d2	s1d2	s1d2	S1D2	S1D2	S1D2	S1D2	S1D2	S1D2	S1D2	s1d2	S1D2	S1D2	s1d2	s1d2	137c	137c	137c
		0.5	0.5	0	0	0	0	0	0	0	0	0	0	0	0	0	0.5	0.5	0.5	0.5
		0			0	0	0	0	0	0	0	0	0	0	0	0	0.5	0	0	0
ADP2	D3	137c	137c	137c	137c	137c	137c	137c	137c	137c	137c	137c	137c	137c	137c	137c	137c	137c	s1d2	S1D2
WT	D4	137c	137c	S1D2	S1D2	S1D2	S1D2	S1D2	S1D2	S1D2	S1D2	S1D2	s1d2	S1D2	S1D2	s1d2	s1d2	s1d2	s1d2	S1D2
WT	D6	S1D2	S1D2	S1D2	S1D2	S1D2	S1D2	S1D2	S1D2	S1D2	S1D2	S1D2	s1d2	S1D2	S1D2	s1d2	s1d2	s1d2	s1d2	137c
ADP2	GHOST	S1D2	S1D2	137c	137c	137c	137c	137c	137c	137c	137c	137c	137c	137c	137c	137c	137c	137c	137c	137c
		0.5	0.5	0	0	0	0	0	0	0	0	0	0	0	0	0	0	0	0	0.5
		0	0.5	0	0	0	0	0	0	0	0	0	0	0	0	0	0.5	0	0	0

Table 3-3: Linkage Analysis of the 63 progeny from the *adf2-1/S1D2* bulk-zygote analysis

Zygotes from an *adf2-1/S1D2* cross were germinated in bulk and then plated. From this plating 250 colonies were assayed for deflagellation- of the 250 strains phenotypes could only be assigned to 63 strains. Linkage analysis was performed on the strains using the following molecular markers: 1.5B, CNA34, 6A, 7A, 8B, and 8.5B. S1D2: indicates the presence of the polymorphic genotype (green); 137c: indicates the presence of the non-polymorphic genotype (blue); WT: indicates the wild type deflagellation state (orange); ADF2: indicates the *adf2* mutant deflagellation state/phenotype (purple); Total: indicates the recombination frequency between the ADF2 phenotype and the molecular markers. Blank cells indicate missing genotypes.

Phenotype	Strain	1.5B	CNA34	6A	7A	8B	8.4A	8.5B
adf2	13	137c	137c	137c	137c	137c	137c	137c
adf2	23	137c	137c	137c	137c	137c	137c	137c
adf2	45	137c	137c	137c	137c	137c	137c	137c
adf2	65	137c	137c	137c	137c	137c	137c	137c
adf2	67	137c	137c	137c	137c	137c	137c	137c
adf2	70	137c	137c	137c	137c	137c	137c	137c
adf2	90	137c	137c	137c	137c	137c	137c	137c
adf2	95	137c	137c	137c	137c	137c	137c	137c
adf2	96	137c	137c	137c	137c	137c	137c	137c
adf2	99	137c	137c	137c	137c	137c	137c	137c
adf2	106	137c	137c	137c	137c	137c	137c	137c
adf2	111	137c	137c	137c	137c	137c	137c	137c
adf2	115	137c	137c	137c	137c	137c	137c	137c
adf2	132	137c	137c	137c	137c	137c	137c	137c
adf2	133	137c	137c	137c	137c	137c	137c	137c
adf2	135	137c	137c	137c	137c	137c	137c	137c
adf2	136	137c	137c	137c	137c	137c	137c	137c
adf2	144	137c	137c	137c	137c	137c	137c	137c
adf2	160		137c					
adf2	167	137c	137c	137c	137c	137c	137c	137c
adf2	188	137c	137c	137c	137c	137c	137c	137c
adf2	190	137c	137c	137c	137c	137c	137c	137c
adf2	191	137c	137c	137c	137c	137c	137c	137c
adf2	197	137c	137c	137c	137c	137c	137c	137c
adf2	213	137c	137c	137c	137c	137c	137c	137c
adf2	214	137c	137c	137c	137c	137c	137c	137c
adf2	226	137c		137c	137c	137c	137c	137c
adf2	228		137c	137c	137c	137c	137c	137c
wt	1	s1d2	s1d2			s1d2	s1d2	s1d2
wt	24	s1d2	s1d2	s1d2	s1d2	s1d2	s1d2	s1d2

wt	48	s1d2	s1d2	s1d2	s1d2	s1d2	s1d2	s1d2
wt	55	s1d2	s1d2	s1d2	s1d2	s1d2	s1d2	s1d2
wt	56	s1d2	s1d2	s1d2	s1d2	s1d2	s1d2	s1d2
wt	57	s1d2	s1d2	s1d2	s1d2	s1d2	s1d2	s1d2
wt	103	s1d2	s1d2	s1d2	s1d2	s1d2	s1d2	s1d2
wt	121	s1d2	s1d2	s1d2	s1d2	s1d2	s1d2	s1d2
wt	124	s1d2	s1d2	s1d2	s1d2	s1d2	s1d2	s1d2
wt	128	s1d2	s1d2	s1d2	s1d2	s1d2	s1d2	s1d2
wt	131	s1d2	s1d2	s1d2	s1d2	s1d2	s1d2	
wt	134	s1d2	s1d2	s1d2	s1d2	s1d2	s1d2	s1d2
wt	138	s1d2	s1d2	s1d2	s1d2	s1d2	s1d2	s1d2
wt	189	s1d2	s1d2	s1d2	s1d2	s1d2		
wt	15	s1d2	s1d2	s1d2	s1d2	s1d2	s1d2	s1d2
wt	17	s1d2	s1d2	s1d2	s1d2	s1d2	s1d2	s1d2
wt	*22	s1d2	s1d2	s1d2	s1d2	137c	137c	s1d2
wt	28	s1d2	s1d2	s1d2	s1d2	s1d2	s1d2	s1d2
wt	36	s1d2	s1d2	s1d2	s1d2	s1d2	s1d2	s1d2
wt	53	s1d2	s1d2	s1d2	s1d2	s1d2	s1d2	s1d2
wt	77	s1d2	s1d2	s1d2	s1d2	s1d2	s1d2	s1d2
wt	80	s1d2	s1d2	s1d2	s1d2	s1d2	s1d2	s1d2
wt	119	s1d2	s1d2	s1d2	s1d2	s1d2	s1d2	s1d2
wt	137	s1d2	s1d2	s1d2	s1d2	s1d2	s1d2	s1d2
wt	139	s1d2	s1d2		s1d2	s1d2	s1d2	s1d2
wt	142	s1d2	s1d2		s1d2	s1d2	s1d2	s1d2
wt	153	s1d2	s1d2	s1d2	s1d2	s1d2	s1d2	s1d2
wt	154	s1d2	s1d2	s1d2	s1d2	s1d2	s1d2	s1d2
wt	155	s1d2	s1d2	s1d2	s1d2	s1d2	s1d2	s1d2
wt	174	s1d2		s1d2	s1d2	s1d2	s1d2	s1d2
wt	177	s1d2		s1d2	s1d2	s1d2	s1d2	s1d2
wt	178	s1d2		s1d2	s1d2	s1d2	s1d2	s1d2
wt	180	s1d2		s1d2	s1d2	s1d2	s1d2	s1d2
wt	194	s1d2	s1d2	s1d2	s1d2	s1d2		
wt	220	s1d2	s1d2	s1d2	s1d2	s1d2		
Total		0	0	0	0	0.015	0.015	0

References

Finst RJ, Kim PJ, Quarmby LM: Genetics of the Deflagellation Pathway in Chlamydomonas. *Genetics* 149: 927-936, 1998

Kathir P, LaVoie M, Brazelton WJ, Haas NA, Lefebvre PA, Silflow CD: Molecular map of the Chlamydomonas reinhardtii nuclear genome. *Eukaryot Cell* 2: 362-379, 2003

Lewin RA, and Burrascano C: Another new kind of Chlamydomonas mutant, with impaired flagellar autotomy. *Experientia* 39: 1397-1398, 1983

4. Discussion

Calcium signalling pathways are key to many signal transduction events. For the ciliated green alga *Chlamydomonas reinhardtii* calcium signalling is important for proper flagellar function (Yang et al., 2011, King, 2010, Tsiokas, 2009). Flagellar autotomy, or deflagellation, is a calcium dependent process in which cells sever their flagella in response to stress signals. Though the mechanism for deflagellation remains to be elucidated the process has been observed in a variety of ciliated eukaryotic cells.

One way to induce deflagellation is by treating cells with weak organic acids, which lower the cytosolic pH activating a flux of extracellular calcium into the cell (Quarmby & Hartzell, 1994). Once in the cell the extracellular calcium causes the release of calcium from intracellular stores, which activates the microtubule severing machinery achieving axonemal severing at the site of flagellar autotomy. Using *Chlamydomonas reinhardtii* as a system to study deflagellation two mutagenesis screens were performed for deflagellation defective mutants. Using UV and insertional mutagenesis, three genes were discovered in the First screen in 1998: ADF1, FA1 and FA2 (Finst et al., 1998). A second UV mutagenesis screen was performed fourteen years later for conditional deflagellation mutants; to date only 1 confirmed novel gene, ADF2, was generated in this second screen. Characterization of the FA genes reveal that they encode members of the microtubule severing machinery, while the ADF genes are involved in the proton-activated calcium-signalling pathway responsible for the activation of the severing machinery.

4.1 ADF1

The first *adf* mutant, *adf1-1*, was originally identified as an unlinked mutation in a secondary screen for deflagellation mutants in mating defective strains. Though unable to deflagellate in response to weak organic acids, *adf1* mutants can deflagellate if the proton-activated calcium flux is bypassed by permeabilizing the cells in the presence of calcium through detergent treatment (Quarmby & Hartzell, 1994). This calcium influx is missing in *adf1* mutants indicating that ADF1 encodes a proton-sensitive protein, like a proton-activated ion channel or the protein that activates the channel. To identify the ADF1 gene I performed complementation analysis using WT DNA from the ADF1 gene locus. Using this approach I recovered what appears to be a suppressor of *adf1*. Several methods were taken to identify the DNA flanking the selectable marker used to generate the suppressor, but they were all unsuccessful. As I was unable to rescue *adf1* with WT DNA from two of the sub-regions in the ADF1 locus, it is likely that ADF1 lies in the third sub-region: the 50kb sequence gap.

The next step in the search for ADF1 would be to try and fill in the sequence gap. The Quarmby lab is currently doing this by using PACBIO RS II de novo assembly to sequence through the 50kb gap (Pacific Biosciences, Pullman, USA). The PACBIO RS II system is based on single-molecule, real-time sequencing (SMRT) technology, in which DNA synthesis occurs in SMRT cells containing thousands of well-like containers with each well containing a single molecule of DNA and a single immobilized polymerase. During DNA synthesis, only the fluorescence that occurs when a labeled nucleotide is incorporated into the synthesizing strand is detected. Following incorporation, the fluorescent label is then removed from the nucleotide leaving the strand unmodified. This technology allows for the generation of long reads and is unbiased to GC content, making

it possible to sequence and assemble regions with high GC content and repetitive sequences. Using this technology we hope to assemble reads to the 50kb sequence gap thereby creating a reference of the gap in a wild type strain (137c). Illumina sequencing (which generates more reads at the fraction of the price of PACBIO) could then be performed on the *adf1* alleles to identify nucleotide polymorphisms between the 137c reference genome and those of the *adf1* alleles. This might lead to the discovery of candidate genes in the 50kb gap that could then be used in phenotypic rescue assays to identify the ADF1 gene.

The identification of the flanking DNA in the *adf1-3* rescue strain also needs to be performed in order to determine if the PAR marker was inserted in a novel gene (*adf1* suppressor) or near BAC24114 DNA. The discovery, and subsequent characterization, of a suppressor could give us insight into the calcium-signalling pathway in deflagellation. Through protein interaction assays, such as immunoprecipitation, substrates/protein partners of the suppressor could be identified- potentially allowing us to determine members of the proton activated calcium-signalling pathway, like ADF1. Though the data indicates that the *adf1-3* rescue strain is a suppressor we cannot yet rule out it being a rescue. It is possible that the PAR marker integrated into the genome along with a fragment of BAC24114, which carried the ADF1 gene. Though over 2000 transformants were assayed with wild type DNA covered by this BAC, these transformants may not have carried the fragment in which ADF1 gene is on. If this is the case then gene prediction 56 (g9856) is of high interest. In a whole-genome transcriptome study, that analyzed genes up-regulated during ciliogenesis, eight of the 49 predicted genes in the ADF1 gene locus were found to be up-regulated following deflagellation (Albee et al., 2013). Among the eight predicted genes is g9856, the transient receptor/potential ion channel protein present in BAC24114. It is therefore important that we identify the DNA flanking the PAR insertion

site to determine if the *adf1-3* rescue strain is a suppressor or a real rescue. Methods such as: direct genomic sequencing, AIMS PCR (Frey et al., 1998), or DLA-Based strategies (Liu et al., 2009), could be employed to identify the flanking DNA of the PAR insertion.

4.2 ADF2

The recovery of a second acid deflagellation gene, ADF2, further expands the proton activated calcium-signalling pathway in deflagellation. Linkage analysis places the ADF2 gene locus on either: (1) a 437.8kb region on chromosome 3: 6266545-6695119 or (2) on a 1.4Mb region on chromosome 3: 6704360-8124216 (www.phytozome.net). The 437.8kb region contains 99 predicted genes spanned by 9 major BACs (Figure 4-1). Looking at the proton-activated calcium-signalling pathway we know that the following proteins must be involved in this process: (1) a proton-sensitive protein that either activates a calcium channel or is the calcium channel, and (2) a calcium sensor that perceives the flux of calcium into the cell following acidification. With this in mind, four of the 99 gene predictions stand out: (1) g4036, which has a predicted adenylate/guanylate cyclase catalytic domain, (2) g4039 a voltage-gated shaker-like K⁺ channel, (3) g4050 a centriole protein and (4) g4090, which is a predicted Calmodulin related protein. There are seven other gene predictions, which stand out from this 437.8kb region due to their up-regulation post-deflagellation (Table 4-1) (Albee et al., 2013). The 1.4Mb region contains 3,150 gene predictions, 16 of which are up regulated following deflagellation (Table 4-1). Of these 16 genes three stand out with respect to the calcium-signalling pathway in

deflagellation: (1) g206650 a Calmodulin/Calcium dependent like-kinase, (2) g201200 a flagellar associated protein and (3) g200950, which is also a flagellar associated protein.

Looking at LG III (Figure 4-1), ADF2 maps to the right of the *tua1* mutant; several mutants lie in this region including: *ac17*, *ac141*, *ida3*, *ac207*, *ac210* and *thi2*. Like the ADF1 gene locus, the region that ADF2 maps to also has its obstacles. The mutations in all of these mutants, with the exception of *tua1*, have yet to be identified. In 2012, whole-genome sequencing was performed in the attempts to identify two mutants on LG III: NG30 and *ac17* (Dutcher et al., 2012). NG30 was found to contain a mutation in the IFT80 gene, a component of IFT complex B necessary for ciliogenesis, which is on chromosome 3: 7643613-7649737. Unlike NG30, whole-genome sequencing in combination with linkage analysis failed to identify the *ac17* mutation. The study found that the 676kb region that AC17 maps to not only contains highly repetitive sequences but also lacks an intact scaffold. One of the two possible locations for ADF2 is the AC17 region (chromosome 3: 6840208-7516918). If ADF2 lies in the AC17 region then it is possible that the same difficulties that have prevented the identification of AC17 through bioinformatics may complicate the discovery of the ADF2 gene. Like with ADF1, however, new sequencing technologies such as PACBIO can be employed to create full assemblies of these regions allowing for the identification of genes through whole-genome sequencing.

The recovery of a conditional allele of a new deflagellation gene strengthens our hypothesis that null mutations in the remaining genes involved in deflagellation are not viable. These genes are likely playing other roles in the cell that makes them essential for normal cell function and survival. This would explain why these genes were not recovered in the original 1998 genetic screen. Thus, the identification of ADF2 could allow us to finally determine if there is a link between deflagellation and the axonemal severing event during pre-mitotic reabsorption.



Figure 4-1: LG III molecular and genetic markers.

Left: molecular markers used for Linkage analysis, on Linkage Group (LG) III. Right: genetic markers (mutants) on LG III. The genes responsible for the mutations in the mutants to the right (below) *tua1* have yet to be identified.

Cre03.g193000	chromosome_3:6284963-6287860	HALOACID DEHALOGENASE-LIKE HYDROLASE
Cre03.g193300	chromosome_3:6302482-6305070	Predicted haloacid-halidohydrolase and related hydrolases
Cre03.g193550	chromosome_3:6327470-6329854	39S ribosomal protein L46, mitochondrial
Cre03.g194300	chromosome_3:6403538-6407184	putative phytoene synthase
Cre03.g194350	chromosome_3:6407324-6411091	-
Cre03.g195950	chromosome_3:6570078-6574672	GAG-POL-RELATED RETROTRANSPOSON
Cre03.g197050	chromosome_3:6646340-6648571	histone H3.2
Cre03.g198200	chromosome_3:6758095-6778656	1,3 beta-glucan synthase
g4157	chromosome_3:7241513-7244852	-
Cre03.g206700	chromosome_3:7322749-7329343	-
Cre03.g206650	chromosome_3:7329463-7332792	doublecortin and CaM kinase-like 1, isoform CRA_b
Cre03.g204550	chromosome_3:7601218-7605959	adenosine kinase isoform c
g4224	chromosome_3:7606079-7608651	-
Cre03.g204500	chromosome_3:7608829-7614531	-
Cre03.g204300	chromosome_3:7632407-7636999	-
Cre03.g204250	chromosome_3:7637423-7640886	adenosylhomocysteinase isoform 1
Cre03.g204150	chromosome_3:7643612-7649737	intraflagellar transport protein 80 homolog isoform a
Cre03.g201900	chromosome_3:7972609-7977575	radial spoke head 1 homolog
Cre03.g201600	chromosome_3:8005275-8008197	-
Cre03.g201300	chromosome_3:8057795-8062627	DBH protein
Cre03.g201250	chromosome_3:8062639-8064595	G patch domain-containing protein 8
Cre03.g201200	chromosome_3:8064715-8067537	Hypothetical Flagellar Associated Protein; found in the flagellar proteome [PMID: 15998802]
Cre03.g200950	chromosome_3:8093956-8095662	Flagellar Associated Protein

Table 4-1: Genes up-regulated during ciliogenesis in the ADF2 gene locus.

Transcript expression levels were measured by comparing mRNA levels predeflagellation, 3, 10, 30 and 60 minutes into ciliogenesis. First column: gene prediction ID; second column: genome location; third column: gene annotation. Gene predictions of interest are in pink; those with no annotations are in light green. Gene predictions Cre03.g193000 through Cre03.g197050 lie in the 437.8kb region, the remaining 16 predictions are in the second 1.4Mb ADF2 gene locus Albee et al., 2013.

References

- Albee AJ, Kwan AL, Lin H, Granas D, Stormo GD, Dutcher SK: Identification of cilia genes that affect cell-cycle progression using whole-genome transcriptome analysis in *Chlamydomonas reinhardtii*. *G3 (Bethesda)*: doi: 10.1534/g3.113.006338, 2013.
- Dutcher SK, Li L, Lin H, Meyer L, Giddings TH Jr, Kwan AL, Lewis BL: Whole-genome sequencing to identify mutants and polymorphisms in *Chlamydomonas reinhardtii*. *G3 (Bethesda)*: doi: 10.1534/g3.111.000919, 2013.
- Finst RJ, Kim PJ, Quarmby LM: Genetics of the Deflagellation Pathway in *Chlamydomonas*. *Genetics* 149: 927-936, 1998
- Frey M, Stettner C, Gierl A: A general method for gene isolation in tagging approaches: amplification of insertion mutagenized sites (AIMS). *The Plant Journal* 13: 717-721, 1998
- King SM: Sensing the mechanical state of the axoneme and integration of Ca^{2+} signalling by outer arm dynein. *Cytoskeleton* 67: 207-213, 2010
- Liu S, Dietrich CR, Schnable PS: DLA-Based Strategies for Cloning Insertion Mutants: Cloning the *gl4* Locus of Maize Using Mu Transposon Tagged Alleles
- Quarmby LM, Hartzell HC: Two distinct, calcium-mediated, signal transduction pathways can trigger deflagellation in *Chlamydomonas reinhardtii*. *J Cell Biol* 124: 807-815, 1994
- Tsiokas L: Function and regulation of TRPP2 at the plasma membrane. *Am J Physiol Renal Physiol* 297: F1-F9, 2009

Yang Y, Cochran DA, Gargano MD, King I, Samhat NK, Burger BP, Sabourin KR, Hou Y, Awata J, Parry DA, Marshall WF, Witman GB, Lu X: Regulation of flagellar motility by the conserved flagellar protein CG34110/Ccdc135/FAP50. *Mol Biol Cell* 22: 976-987, 2011

5. Materials and Methods

5.1 Strains and Growth conditions

The *Chlamydomonas reinhardtii* strain S1D2 was obtained from the Chlamydomonas Resource Center (University of Minnesota, USA). All strains were maintained on TAP (Tris-Acetate-Phosphate) solid media under constant illumination at 21°C.

5.2 BAC DNA & Plasmid Preparations

The Quiagen Plasmid Maxi Kit (Valencia, USA) was used to prepare BAC DNA from the *Chlamydomonas* BAC library (Chlamydomonas Resource Center, University of Minnesota, USA). BAC DNA was resuspended in 500uL sterile dH₂O following extraction. Plasmid DNA was prepared using a modified protocol from Molecular Cloning (Sambrook & Russell, 2001). Bacteria were grown in 2mL of rich media (LB), pelleted then resuspended in 150uL of 10mM EDTA and 5mg of Lysozyme from chicken extract (Sigma, St. Louis, USA) and incubated for 2 minutes at room temperature. A 250uL solution of 1% SDS and 200mM NaOH was then added followed by a 3-minute incubation period (at room temperature). A chloroform:IsoAmyl Alcohol (49:1) extraction was then performed by first adding 150uL of 4M Potassium Acetate followed by 300uL of the chloroform:IsoAmyl alcohol. The extracted plasmid DNA was then washed with 70% ethanol and resuspended in 100uL sterile water.

5.3 Sub-cloning for phenotypic assays and for sequencing

Gene predictions 71-75 (from the 40kb region of the ADF1 locus) were subcloned by Ziwei Ding and Adam Staniscia into pSI103 by first amplifying the predictions from genomic DNA then ligating them into the vectors. Self-ligation PCR, TAIL-Adaptor PCR and the PAR

insertion sites (6.5kb SmaI and 7.6kb HindIII bands) were sub-cloned into pGEMT or pBlueScript SK- by restriction digest. The inserts were ligated at a 5:1 insert to vector mole ratio in 20uL reactions with 1 unit of T4 DNA ligase from New England Biolabs (NEB, Ipswich, USA), prior to transformation into bacteria.

5.4 *Chlamydomonas* transformations

Chlamydomonas adf1 mutant cells were transformed with BAC DNA or plasmids for phenotypic rescue assays using a modified protocol from Kindle, 1990. The *adf1* strains were first grown in 150mL liquid TAP under constant illumination and shaking at 21°C for two days. Cell concentration was then measured using a hemocytometer. The cells were then pelleted (800xg for 5 minutes), resuspended in GLE (gametic lytic enzyme, 15mL) and incubated under constant illumination and shaking at 21°C for 90 minutes to digest the cell wall.

Transformations were done in 15mL Falcon tubes: autoclaved Next Advance glass beads (0.5mm diameter, Averill Park, USA) were loaded into the tubes and the DNA (digested BAC or plasmid, 500ng, plus 200ng pSI103) was then added to the wall of the tube around the 7mL marker. The cells were then centrifuged as before and resuspended in liquid TAP to a total concentration of 3.3×10^8 cells/mL. 300ul of cells were then added to the Falcon tubes (making sure they contacted the DNA) and 100uL of 20% PEG (polyethyleneglycol, MW 8000). The cells were then allowed to sit for 5 minutes before vortexing for 30 seconds. Fresh TAP (10mL) was then added and vortexed again after a 5 minute sit period.

The cells were then transferred to a new Falcon tube making sure that no beads were transformed. They were then incubated overnight shaking under the lights at 21°C. The following day the cells were pelleted, resuspended in 500mL TAP and plated on TAP media containing paromomycin with sterile loops. Colonies were recovered ~5 days after plating and incubation under constant light at 21°C.

5.5 Deflagellation Assays

Phenotypic deflagellation assays were carried out in 96-well plates. The wells were filled with 150uL TAP and inoculated with ~10uL cells (scraped from patch-plates with toothpicks), and placed under constant shaking and illumination at 21°C overnight for transformed *adf1* cells. For *adf2* phenotypic assays the 96-well plates were prepared in the same way, but following the overnight incubation they were incubated at 33°C for 8 hours. Deflagellation assays were then performed either on microscope slides or in the 96-well plates. Assays were done by treating cells with equal volume of acid deflagellation buffer (containing 40mM Na Acetate and 1mM CaCl₂, pH 4.5) for 30 seconds, then fixing the cells with equal volume of 2.5% glutaraldehyde. Deflagellation was assessed through light microscopy.

5.6 Genetic crosses

Chlamydomonas strains were mated using the protocol from The Chlamydomonas Sourcebook (Ed. Harris, 2009) with some modifications. Strains with opposite mating type (+ or -) were first plated separately on 1.5% LOW-N (low nitrogen) TAP plates for 2-3 days under constant light at 21°C, to induce gametogenesis. The cells were then harvested and resuspended in liquid LOW-N TAP, then placed in a shaker for 1-2 hours, until flagella were fully generated. Equal volumes of gametes were then added to 24-well plates and placed under bright lights, without shaking, at 21°C and assessed for quadriflagellate cells (dikaryons). Once quadriflagellates had been observed the mating was plated on 4% TAP plates (700uL per plate) and the plates were allowed to dry overnight at 21°C. The following day the plates were wrapped and incubated in the dark for 3-5days at 16°C.

Zygotes were recovered by scraping vegetative cells off with a sterile blade. Zygotes were then handpicked with a glass pipet needle and transferred to a 1.5% washed-TAP plate (into gridded boxes imprinted on the plate). Meiotic tetrads were then separated using glass needles under a dissecting microscope. The resulting colonies were then patch-plated on 1.5% TAP. The colonies were then screened for various phenotypic traits such as deflagellation, resistance to oryzalin, acetate requirements and p-aminobenzoic acid requirements.

5.7 Genomic DNA isolation from *Chlamydomonas*

An Arabidopsis plant DNA extraction protocol was used to extract genomic DNA from *Chlamydomonas* cells for PCR. A loop of cells (~500uL) was incubated in 500uL pre-warmed CTAB buffer (1.4M NaCl, 20mM EDTA pH8, 100mM Tris-HCl pH8, 3% CTAB) and proteinase K (20mg/ml) at 65°C for 60 minutes. Upon removal from the water bath, they were briefly vortexed and 500uL of 24:1 chloroform:isoamyl alcohol was added and mixed by shaking for 30 seconds. The cells were then centrifuged at 14,000xg for 10 minutes. The aqueous layer was then transferred into a new tube with 500uL of 1M Ammonium acetate in isopropanol, and mixed gently by inversion. A second centrifugation was then performed for 6 minutes and the pellet was then washed with 70% ethanol. The pellet was then RNase A treated then resuspended in 200uL sterile dH₂O.

5.8 Southern Blots

Southern blots were performed as described in Molecular Cloning (Sambrook & Russell, 2001) with some modifications. 50ug genomic DNA was digested overnight in 40uL reactions with 3 units of restriction enzymes. The digested DNA was then run on a 0.4% 500mL 0.5XTBE agarose gel at 120V for 5-6 hours. Depurination was then performed by soaking the gel in 0.24M HCL for 15 minutes, shaking. Transfer of DNA to the positively charge Zeta-Probe nylon membrane from BioRad (Hercules, USA) was performed according to the alkaline blotting (DNA capillary transfer) protocol from BioRad. Following transfer, the membrane was rinsed in 2XSSC, air dried, then baked at 80°C for 1 hour.

Probes were either randomly labeled with [α -³²P] dCTP (6000Ci/mmol, BLU013Z500UC, Perkin Elmer) or by end-labeling with [γ -³²P] dCTP. Random labeling was performed using protocol from the Takara Ladderman Labeling Kit (Mountain View, USA). 50ng of template DNA was used in the reaction. The PAR southern blot and colony lifts were performed with end-labelled probes. End-labeling was done by incubating 100ng template DNA with 10uL of isotope, 5uL 5X priming buffer (350mM Tris-HCl, 50mM MgCl₂, 500mM KCl, 5mM 2-mercaptoethanol) and 1 unit of Polynucleotide kinase from Invitrogen (Burlington, Canada) for 3 hours at room temperature. Unincorporated isotope was removed by using Fermentas GeneJet PCR purification kit (Ottawa, Canada).

Prior to hybridization, the membranes were pre-hybridized in hybridization buffer (1% SDS, 5X SSPE, 20% Formamide, 1X Dehardt's solution) at 42°C for 2 hours. Fresh buffer

(10mL) was then added along with the isotope (1-2x10⁶ cpm/mL) and incubated at 42°C overnight with agitation. The following day the membrane was washed with wash solution (1X SSPE, 0.5% SDS) four times, each for 30 minutes at room temperature. Membranes were then exposed to either film (overnight) or a phosphoimager screen (2-5 hours).

5.9 TAIL-Adaptor PCR

The TAIL-Adaptor PCR was carried out according to the protocol by Iomini et al., 2009. The plus and minus adaptors were ligated to each other (25uM each) in a 50uL reaction and stored at 4°C. The adaptor (1.25 uM) was then ligated to the 6.5kb SmaI and 7.5kb HindIII PAR insertion bands in a 20uL reaction at 16°C overnight. Two nested PCRs were then performed: (1) using the RIM3-1 and AP1 primer set and (2) using the RIM3-2 and AP2 primer set. The PCRs were carried out in 50uL volumes containing: 2uL 10mM dNTPs, 2.5uL 100% DMSO, 0.125uL of the forward and reverse primers (100uM), 5uL 10X Thermopol buffer, 2.5uL 50mM MgCl₂ and 0.25uL Taq DNA Polymerase (from New England Biolabs, with 10X Thermopol buffer). For the first nested PCR 2uL of the ligation reaction (adaptor + PAR insertion bands) was used (the ligation was first diluted to 50uL prior to using), 5uL of this PCR was then used for the second nested PCR. Touchdown PCR cycling conditions were used for both nested PCRs (below). Following the second nested PCR the product was gel extracted using the QIAquick gel extraction kit from Qiagen, and then ligated into pGEMT prior to sequencing.

95°C → 3 minutes	
95°C → 30 seconds	
70°C → 8 minutes	} X 5
72°C → 6 minutes	
95°C → 30 seconds	
65°C → 8 minutes	} X 25
72°C → 6 minutes	
72°C → 5 minutes	
4°C → hold	

5.10 Self-ligation PCR

For the Self-ligation PCR method the 6.5kb SmaI and 7.5kb HindIII PAR insertion bands were individually allowed to self-ligate in 20uL reactions with 1 unit of NEB T4 DNA ligase (Whitby, Canada), overnight at 16°C. The ligation reactions (5uL) were then digested with

1 unit of NEB BamHI in 20uL reactions for 1 hour at 37°C then incubated at 65°C for 20 minutes to heat-inactivate the restriction enzyme. PCR was then performed using the PAR+ primer as the forward primer and TPA1R as the reverse primer (which binds to the backbone of pSI103). The PCR recipe was the same as that used for TAIL-Adaptor PCR (Iomini et al., 2009), except that the ligation reaction was not diluted prior to PCR and 5uL of the reaction was used in the PCR. Touchdown PCR cycling conditions were used (below). The PCR product was then gel extracted using the QIAquick gel extraction kit from Qiagen (Valencia, USA) and ligated into pGEMT prior to sequencing.

95°C → 3 minutes	
95°C → 30 seconds	} X 10
70°C → 7 minutes	
72°C → 6 minutes	
95°C → 30 seconds	} X 20
65°C → 7 minutes	
72°C → 6 minutes	
72°C → 5 minutes	
4°C → hold	

5.11 Bacterial transformations

Chemically competent Mach1 *E. coli* were transformed by heat shock using the Inoue Method for Preparation and Transformation of Competent *E. coli*: Ultra-Competent cells (Molecular Cloning, Sambrook & Russell, 2009). Cells (50uL) were incubated with plasmids/constructs for 30 minutes on ice prior to heat shocking at 42°C for 60 seconds. 250uL LB media (lysogeny broth) was then added and the cells were incubated at 37°C for 1 hour with shaking (250rpm). The cells were then pelleted (5000xg for 2 minutes) and the pellet resuspended in 100uL LB and plated (on solid LB media with antibiotics- if needed).

5.12 Colony lifts


Colonies were transferred onto a MSI Magna nylon transfer membrane using a modified protocol from Molecular Cloning (Sambrook & Russell, 2001). The membrane was first placed on top of the colonies, peeled off, placed in a petri dish containing 0.5M NaOH for 10 minutes then transferred to a stack of Whatman paper to remove the excess NaOH. The membrane was then soaked in a 0.5M Tris-Cl pH 8, 0.5M NaCl solution, dried, and

then soaked in 2X SSPE. The DNA was then fixed by baking the membrane at 80°C for 1 hour. Probes for hybridization were labeled by end-labeling and hybridized as was done for the southern blot membranes (see Section 5.8).

5.13 PCR-based recombination frequency mapping

Progeny from 9 zygotes were recovered and assayed for the ADF2 phenotype; genomic DNA extractions were then performed for PCR. The Kit for Molecular Mapping of *Chlamydomonas* Genes version 1.1 (*Chlamydomonas* Resource Centre, University of Minnesota) was used for mapping (Kathir et al., 2003). The primers were ordered in bulk from Eurofins mwg operon (50nmol) (Huntsville, USA). The PCR reaction mix contained: 80% glycerol, 0.8% Formamide, 23% GoTaq Buffer, 10uM Primers, 10mM dNTPs, 50ng DNA, 0.25uL GoTaq DNA polymerase (Promega, Madison, USA) in a 30uL reaction. The general cycling conditions for the molecular markers of the kit is seen below, x indicating the annealing temperature of the primers. PCR reactions were run on 1% or 3% agarose gels at 120V for 1-2 hours.

94°C → 2 minutes
94°C → 1 minute
X°C → 1 minute
72°C → 1 minute
4°C → hold



X 40

References

- Harris EH: Chlamydomonas in the Laboratory, in: The Chlamydomonas Sourcebook: Introductions to Chlamydomonas and Its Laboratory Use, 2nd Edition. Academic Press. 2009
- Iomini C, Till JE, and Dutcher SK: Genetic and Phenotypic Analysis of Flagellar Assembly Mutants in Chlamydomonas reinhardtii. *Methods in Cell Biology* 93: 121-143, 2009.
- Kathir P, LaVoie M, Brazelton WJ, Haas NA, Lefebvre PA, Silflow CD: Molecular map of the Chlamydomonas reinhardtii nuclear genome. *Eukaryot Cell* 2: 362-379, 2003
- Kindle KL: High-frequency nuclear transformation of Chlamydomonas reinhardtii. *Genetics* 87: 1228-1232, 1990
- Sambrook J and Russell D: Protocol 1: Preparation of Plasmid DNA by Alkaline Lysis with SDS: Miniprep. In: *Molecular Cloning*, 3rd Edition. Cold Spring Harbor Laboratory Press. 2001
- Sambrook J and Russell D: Protocol 10: Southern Hybridization of Radiolabeled probes to Nucleic acids Immobilized on Membranes. In: *Molecular Cloning*, 3rd Edition. Cold Spring Harbor Laboratory Press. 2001
- Sambrook J and Russell D: Protocol 24: The Inoue Method for Preparation and Transformation of Competent E. Coli: "Ultra-Competent" Cells. In: *Molecular Cloning*, 3rd Edition. Cold Spring Harbor Laboratory Press. 2001
- Sambrook J and Russell D: Protocol 21: Transfer of Bacteriophage DNA from Plaques to Filters. In: *Molecular Cloning*, 3rd Edition. Cold Spring Harbor Laboratory Press. 2001

Appendices

Appendix A. Strains used in this study.

Strain	Phenotype	Maintained on
<i>adf1</i> alleles	Unable to deflagellate in response to acid	1.5% TAP
137c	Wildtype strain	1.5% TAP
S1D2	Polymorphic mapping strain	1.5% TAP
<i>adf2-1</i>	Unable to deflagellate in response to acid at 33°C	1.5% TAP at 21°C

Appendix B. The BACs spanning the ADF1 locus

BAC	Chromosomal location	Gene predictions
17I18	4568281-4590505	33-34
34M13	4589045-4613004	35-37
22N9	4589044-4672504	35-44
1F13	4678343-4709077	47-52
24I14	4672508-4786271	45-60
16D2	4712514-4726541	54-55
34H15	4712977-4805219	54-60
21J15	4786420-4868574	61-70
34C24	4805222-4828672	62-64
14I19	4828634-4868574	66-70

BACs were obtained from *Chlamydomonas reinhardtii* version 4 of the genome browser (Joint Genome Institute, genome.jgi-psf.org/Chlre4/Chlre4.home.html). Chromosomal location of each BAC is given based on the current genome browser (Phytozome, www.phytozome.net). Augustus 10 gene predictions for each BAC are given.

Appendix C. Primers used in the ADF1 Analysis

Gene ID	Location	FWD	REV	Product
g9847	4678915 - 4680920	ggctcaacctggtctactcg	gactcggagctcggtaacag	1814bp
g9848	4680975 - 4683620	tctgctattgcaccactcg	tccagcagaatggattaggg	1279bp
PAR	pSI103	cgggagttgtttgtcaaggt	tcgtccagatcctccaagtc	688bp

The primers were used to generate the template DNA for the Southern blot primers. Chromosomal locations are for the *Chlamydomonas reinhardtii* version 5 of the genome browser (Phytozome, www.phytozome.net).

Primer Name	Sequence	Target
(+) Adaptor	GTAATACGACTCACTATAGAGTACGCGTGGTCGACGGCCCCGGGCTGGT	-
(-) Adaptor	[Phos]ACCAGCCCGG[SP~3]X7[AmC7~Q]	-
RIM3-1	CGGTATCGGAGGAAAAGCTG	PAR
RIM3-2	GCTGTTGGACGAGTTCTTCTG	PAR
AP1	GTAATACGACTCACTATAGAGT	(+) Adaptor
AP2	ACTATAGAGTACGCGTGGT	(+) Adaptor

The primers were used in TAIL-Adaptor PCR

PAR+	GAGGAAAAGCTGGCGTTTTAC	PAR
TPA1R	ACCTTGACAAACAACCTCCCG	pSI103

The primers were used in Self-ligation PCR

Appendix D. Molecular Markers for ADF2 Linkage Analysis

Name	Gene	Location	FWD	REV	Tm	Time	Product	Enzyme	137c	S1D2
5B	g182750	5216867	TGATGCGC TACAACGAC TTC GCTGTATGT CATTGCGCT	AGCAGGCG GTAAGAAG ACAG TCGTAACAC AGCTCGTC	60°	30	896BP	MspI	500	300
3A	g191500	6076708	GT TGTATGTGT GCCGATGT	GTC GCTCGATG TAGCGGAT	60°	30	970bp	MspI	500	650
2A	g192850	6266545	GTG TTCCTGGA GCAAAACCT	GAG AGCTGAAC ACGTCGGA	60°	30		-	650	1000
1.5B	g194100	6377470	GTC GGACTGCA ACCGGAAA	CTTT TCAAACGTG TCCACGTCA	60°	60	884bp	MspI	250, 150	300, 150
1A	g194400	6411156	CTTA GTGGATGG AAGTGGCG	AT TCGTCGTC GTAGATGT	60°	60	742bp	HhaI	300, 150	150
6A	g195366	6525723	AGT ATGTGGGA TGCAGGAA	GCTC CAGCACCA GCAAGAGT	60°	30	726bp	HaeIII	100	100
7.1A	g195700	6551101	TTGT GCATCTGA GAGCGATG	ACCA ATAACGCAC CAGTCCCA	60°	60	915bp	HhaI	350, 200	400, 200
7A	g196450	6604273	ATGA TCTCTGTGG TTGCTGGTC	GTC GCAAGGTG GAAAAAGC	60°	60	840bp	HaeIII	150	150
8B	g197500	6695119	AC	ACAT	60°	60	1036bp	MspI	700, 150	600, 150
8.4A	g197600	6704360	CCAGTATG GCTGGTGA TCCT	AAGAATCTT GGGTGGTG ACG	60°	60	1163bp	MspI	500, 350, 200, 150	350, 350, 300, 150
8.5B	g206950	7292298	GTTTCCTGC ATGCACTCT CA	CTGCTGCT GTAATCCGT TCA	60°	60	1151bp	MspI	350	700, 400
9A	g200750	8124216	CCTAGCAA CCGTTGTC CATT	TGCGCAAC ATACCTATT CCA	60°	60		-	874	0
KINA	g200600	8143186	CACGCGGC AAGACTAC GGCGAC	TCTCGTATC GCCTCCGC GGATAGAG	60°	30		-	500, 200	200
			TGCAGGGCATAGCAGCAAG AGGGAC							

Molecular markers were generated by amplifying ~1kb introns from the Augustus 10 gene predictions (Phytozome, www.phytozome.net), then digesting them with restriction enzymes. Restriction digests were performed at 37°C for 2 hours. Tm: primer annealing temperature; Time: primer annealing time in seconds; FWD: sequence of the forward primer; REV: sequence of the reverse primer; Product: size (bp) of PCR product generated by the primers; Enzyme: restriction enzyme used to digest the PCR; 137c: restriction

bands generated in the non-polymorphic strain 137c; S1D2: restriction bands generated in the polymorphic mapping strain S1D2.